Electronic Predistortion Strategies For Directly Modulated Laser Systems

vorgelegt von
Diplom-Ingenieur
Stefan Warm
aus Berlin

von der Fakulät IV - Elektrotechnik und Informatik
der Technischen Universität Berlin
zur Erlangung des akademischen Grades

Doktor der Ingenieurswissenschaften
- Dr.-Ing. -

genehmigte Dissertation

Promotionsausschuss:

Vorsitzender:	Prof. Dr. Tillak
Berichter:	Prof. Dr. Petermann
Berichter:	Prof. Dr. Krummrich

Tag der wissenschaftlichen Aussprache: 03. April 2009

Berlin 2009
D 83

For
Leo, Louise and Catharina

II

ACKNOWLEDGMENTS

First of all, I would like to thank my wife Catharina and my children Leo and Louise for their patience and understanding during my dissertation.

I would like to thank my supervisors Professor Klaus Petermann and Professor Peter Krummrich for their continued support and the motivating discussions we had.

I also would like to thank my friends and fellow research scholars from the Photonics Group at the Technische Universität Berlin. It was a real pleasure to *work* with you.

Financial support for this work is gratefully acknowledged from the company Nokia–Siemens–Networks.

Stefan Warm
Technische Universität Berlin
September 2009

CONTENTS

CHAPTER 1

INTRODUCTION

Directly modulated lasers (DML) have the advantage of low costs, a small form factor and low power consumption compared to externally modulated lasers. Therefore, directly modulated lasers are widely used in metro systems at the OC-48 rate (2.488 Gb/s) and below. However, at higher data rates in the conventional wavelength range of metro networks (1550 nm), chromatic dispersion limits the maximum transmission distance of conventional non return–to–zero (NRZ) modulated lasers to about 20 km. The reason for this transmission limit is the laser chirp, which leads to a strong broadening of the optical spectrum if the laser is modulated. A few techniques such as dispersion supported transmission (DST) [1] and the chirp managed laser (CML) [2] exist to overcome this inherent transmission limit and allow transmission distances of up to 250 km standard single mode fiber (SSMF).

For externally modulated lasers the standard technique to compensate the effect of chromatic dispersion is the optical dispersion compensation (ODC). Dispersion compensating fibers (DCF) are used after a certain transmission length over SSMF, to compen-

sate the accumulated fiber dispersion. Due to the losses in dispersion compensating fibers, additional fiber amplifiers are necessary, which results in high costs.

Another approach to compensate chromatic dispersion in vector modulated transmission systems is the electronic predistortion (EPD) [3, 4], where the dispersion compensation is done not in the optical, but in the electrical domain. The idea of this technique is to imaginarily propagate a desired signal at the receiver *backwards* through the fiber to the transmitter. A signal that is predistorted in this way and modulated at the transmitter may not be detectable in a *back tot back* case, but after the desired transmission length. Without any optical dispersion compensation, the predistorted signal may be transmitted over several thousand kilometers [3].

In this work the electronic predistortion technique will be adopted to a directly modulated laser system with the intention to overcome the dispersion limit of a directly modulated laser system. Even if the concept is the same, the implementation will be completely different, because direct modulation of a laser cannot modulate its optical intensity and optical phase independently, as it is done with an IQ–modulator. The aim of the work is basically to outperform existing transmission approaches for directly modulated lasers as dispersion supported transmission and the chirp managed laser and thus to make directly modulated lasers applicable for transmission systems which are so far reserved for externally modulated lasers. In order to achieve this, conventional and less conventional approaches in the field of electronic predistortion are studied.

The work is structured as follows: In Chapter 2 the laser diode as a key component of the transmission system is introduced. Beside the general theoretical background of laser diodes, also the modulation characteristics of the laser diode used in this work are presented. Chapter 3 describes physical effects in optical fibers, with emphasis on chromatic dispersion. Chapter 4 gives an overview over existing modulation formats for directly modu-

lated lasers. Beside the standard non return–to–zero modulation format, also more advanced modulation formats such as dispersion supported transmission and the chirp managed laser are reviewed. In Chapter 5 mainly three different approaches for electronic predistortion of directly modulated lasers are discussed: An analytical model, based on a small–signal approximation of the fiber transfer function and the laser modulation characteristic, a finite impulse response (FIR) filter based predistortion and a technique that uses artificial neural networks to obtain the signal predistortion. In Chapter 6 the most promising predistortion technique in this work is combined with signal equalization techniques at the receiver like maximum likelihood sequence estimation (MLSE) or a feed forward / decision feedback filter (FFE/DFE).

CHAPTER 2
LASER DIODES

In optical communication systems, light is used to transmit data signals. Thus, an optoelectronic device to emit this light and a modulator to imprint the telecommunication data onto the light are needed. A laser diode fulfills both requirements as it can directly modulate the light.

2.1. Basic Concept

The concept of a laser[1] is mainly based on the effect of the stimulated emission of light. In contrast to the spontaneous emission, a previously excited electron returns to the ground state not randomly, but due to an incident photon while emitting a photon. The emitted photon has the same energy W and the same propagation characteristic as the incident photon. To obtain laser operation population inversion is required. This means the occupation probability of the conduction band is higher than the occupation

[1] Light Amplification by Stimulated Emission of Radiation

probability of the valance band. At the p-n junction, which is a connection of a p-type and an n-type semiconductor, a population inversion can be obtained with an externally applied forward bias voltage that leads to an electrical current due to carrier diffusion. When the carrier density exceeds the transparency carrier density N_0, the optical power will be amplified. The power amplification can be written as a differential equation:

$$\frac{dP}{dz} = P \cdot g_{st} \tag{2.1}$$

with g_{st} being the gain coefficient due to stimulated emission and P the optical power. The stimulated gain depends on the injected carrier density N and the photon energy $W = h\nu$. It can be linearized related to the carrier density N [5]:

$$g_{st} = a(N - N_0) \tag{2.2}$$

where a is called *differential gain* or *cross section*. However, the active layer in double heterostructure laser is relatively thin and the optical field is only partially confined to the active layer. This is characterized with the confinement factor Γ and the relation: $g = g_{st} \cdot \Gamma$.

In addition to the stimulated emission, there is another important concept for the laser: The optical feedback, which can be provided by a *Fabry–Perot* (FP) cavity (that is why this laser is called a Fabry–Perot laser). With assumed reflectivities R_1, R_2 of two mirrors that form the cavity, the normalized optical power of the signal after one round trip can be described as (see Figure 2.1):

$$P = P_0 \exp(g_{st} L_d) \sqrt{R_1 R_2} \exp(-\alpha_{int} L_d) \tag{2.3}$$

The first term represents the laser gain (in which L_d the laser length), the second term represents the mirror losses and the third

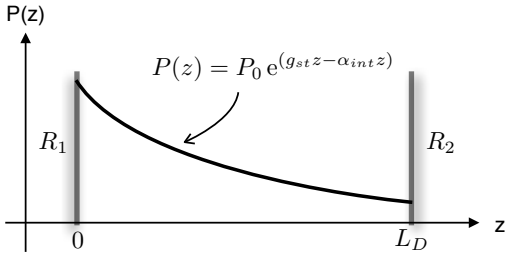

Figure 2.1.: Optical power P of the electromagnetic wave inside the laser cavity

term describes internal losses like scattering and free carrier absorption (with α_{int} being internal losses).

In steady–state, the laser gain is the same as the laser losses and with (2.3) follows:

$$g_{st}(N_{th}) = \alpha_{int} + \frac{1}{2L}\ln\left(\frac{1}{R_1 R_2}\right) = \frac{1}{v_g \tau_p} \tag{2.4}$$

with the threshold carrier density denoted by N_{th}, the photon lifetime τ_p and the group velocity of the light v_g. This condition is also called the lasing condition.

In telecommunication applications, the distributed feedback laser (DFB) is more common than the Fabry–Perot laser described here. In distributed feedback lasers, a refractive index grating close to the active region provides an optical feedback and thus, no mirrors as in the Fabry–Perot laser are necessary. But even if the concept of the distributed feedback laser differs from the concept of a Fabry–Perot laser, the following description is also valid for the distributed feedback laser.

2.2. Modulation Characteristics

In order to describe the small signal modulation characteristics of a laser diode, it is necessary to study the laser rate equation for the photon number S and the carrier density N [5, 6]:

$$\frac{dS}{dt} = \frac{S}{\tau_p}(G-1) + R_{sp} \tag{2.5a}$$

$$\frac{dN}{dt} = \frac{I}{eV} - R(N) - \frac{GS}{\tau_p V}. \tag{2.5b}$$

In these equations, the normalized gain $G = v_g \Gamma \tau_p g_{st}$, the recombination rate of the carrier $R(N)$, the spontaneous emission rate R_{sp} and the injection current I were introduced. V represents the active volume and e the elementary charge.

To analyze the small signal modulation characteristics it is appropriate to consider a sinusoidal modulation of the injection current I around the mean current I_0:

$$I(t) = I_0 + \Re(\Delta I \cdot \exp(j\omega t)) \tag{2.6}$$

with angular modulation frequency ω, the time t and a considered small modulation amplitude $|\Delta I| \ll I_0$. Following this approach, also the photon number S and the carrier density N become sinusoidal with mean values S_0, N_0 and their modulation amplitude $|\Delta S| \ll S_0$, $|\Delta N| \ll N_0$:

$$S(t) = S_0 + \Re(\Delta S \cdot \exp(j\omega t)) \tag{2.7a}$$

$$N(t) = N_0 + \Re(\Delta N \cdot \exp(j\omega t)). \tag{2.7b}$$

Before the rate equations can be linearized, some approximations have to be done. At a high photon density in the active region, gain compression has to be considered, thus the gain compression factor related to the photon number κ_s for the nonlinear gain is introduced:

$$G(N,S) = G_l\,(1 - \kappa_S S) \tag{2.8}$$

where G_l relates to the linear gain. Here, it is appropriate to expand the nonlinear gain (2.8) using the Taylor series:

$$G \approx G(N_0, S_0) + \frac{\partial G}{\partial N}\Delta N + \frac{\partial G}{\partial S}\Delta S \tag{2.9}$$

$$\approx 1 + \frac{\partial G}{\partial N}\Delta N - \kappa_S \Delta S. \tag{2.10}$$

Neglecting the spontaneous emission R_{sp} in steady state, the rate equation for the photon number (2.5a) can be linearized:

$$j\omega\tau_p\ \Delta S = S_0 \left(\frac{\partial G}{\partial N}\Delta N - \kappa_S \Delta S \right). \tag{2.11}$$

In order to linearize the rate equation of the carrier (2.5b) as well, the recombination rate $R(N)$ will be expanded around the mean value of the carrier density N_0:

$$R(N) = R(N_0) + \frac{dR}{dN}\Delta N \tag{2.12}$$

$$= \frac{I_0}{eV} - \frac{GS_0}{\tau_p V} + \frac{\Delta N}{\tau_e}. \tag{2.13}$$

Where τ_e represents the carrier lifetime. Thus, a linearized rate equation for the carrier can be obtained:

$$j\omega\ \Delta N = \frac{\Delta I}{eV} - \frac{\Delta N}{\tau_e} - \frac{S_0}{\tau_p V}\left(\frac{\partial G}{\partial N}\Delta N - \kappa_S \Delta S \right). \tag{2.14}$$

Solving (2.14) for ΔN and then inserting in (2.11) yields the relation between the modulation current ΔI and the modulated photon number ΔS (with use of the relation $(\kappa_S \tau_p)/\tau_e \ll (\partial G/\partial N)/V$)

$$\frac{\Delta S}{\Delta I} = \frac{\tau_p}{e} \cdot H_{LD}(j\omega) \tag{2.15}$$

$$= \frac{\tau_p}{e} \frac{1}{\left(\frac{j\omega}{\omega_r}\right)^2 + \frac{j\omega}{\omega_d} + 1} \tag{2.16}$$

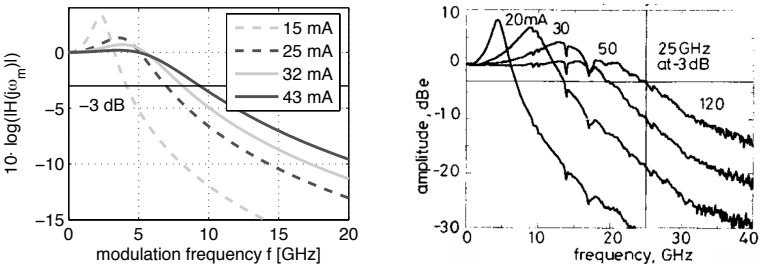

(a) (b)

Figure 2.2.: Small signal laser modulation characteristic in relation to the laser bias current I_{bias}. The theoretical results (a) are based on laser parameters that are used throughout this work (see Appendix A), while the experimental results (b) are from Morton et al. [7].

where ω_r denotes the circular relaxation resonance frequency

$$\omega_r = \frac{1}{\tau_p}\sqrt{\frac{\partial G}{\partial N}\frac{S_0}{V}}, \tag{2.17}$$

and ω_d the damping frequency

$$\frac{1}{\omega_d} = \frac{K}{(2\pi)^2} + \frac{1}{\tau_e \omega_r^2}. \tag{2.18}$$

K is a constant independent of the operating, also known as the "modulation K–factor":

$$\frac{K}{(2\pi)^2} = \tau_p + \frac{\kappa_S \tau_p V}{(\partial G)/(\partial N)} \tag{2.19}$$

In Figure 2.2, theoretical and measured laser transfer functions in relation to the laser bias current I_{bias} are shown. The theoretical transfer functions (Fig. 2.2a) are based on laser parameters

used throughout this work (for detailed parameters see Appendix A). As indicated by (2.17), the relaxation frequency ω_r depends, among other things, on the mean photon number in the active region and therefore can be controlled by the bias current $I_{bias} = I_0$. For a bias current $I_{bias} = 43\,\mathrm{mA}$ as used in Chapter 4.1 to modulate a non return–to–zero (NRZ) modulation, the 3 dB bandwidth of the laser is about 9 GHz. A lower bias current I_{bias} leads to a lower bandwidth. The measured transfer function is from Morton et al. [7] and represents a 1.55 μm GaInAsP multiquantum–well laser with a 3 dB bandwidth of 25 GHz.

Another important aspect of directly modulated lasers is the frequency modulation. Any modulation of the injection current yields to a variation of the carrier density, which leads to a variation of the refractive index and therefore a modulation of the emission frequency.

As for the intensity modulation, for the latter analysis in Chapter 5.1 it is convenient to derive a linearized small signal modulation characteristic of the frequency modulation. For this purpose the rate equation of the frequency is a good starting point [5]:

$$(\nu - \nu_{th}) = \frac{\alpha}{2\pi}\left(\frac{d(\ln S)}{dt} + \frac{1}{\tau_p}\left[\kappa_S S - \frac{n_{sp}}{S}\right]\right) \tag{2.20}$$

with the laser chirp factor (linewidth enhancement factor) α and $(\nu - \nu_{th})$ being the frequency shift of the optical signal. $n_{sp} = R_{sp}/R_{st}$ with R_{st} the stimulated emission rate, is the inversion factor Based on this equation, the spectral broadening due to the laser modulation can be described. The first term in (2.20) is also called the transient chirp, while the second term is called the adiabatic chirp. As will be described later (Chapter 3), this broadening of the optical laser spectrum results in a reduced transmission reach of the optical signal due to pulse spreading induced by chromatic dispersion. Therefore, in standard transmission systems using a directly modulated laser, the chirp factor α should be as low as possible.

For a small signal approach, the frequency modulation may be written as a sinusoidal signal:

$$\nu = \nu_0 + \Re\left(\Delta\nu \cdot \exp(j\omega t)\right). \tag{2.21}$$

Assuming $S_0 \gg \Delta S$, from (2.21) and (2.20) follows:

$$\frac{\Delta\nu}{\Delta S} = \frac{\alpha}{4\pi S_0}\left(j\omega + \omega_g\right) \tag{2.22}$$

with the characteristic frequency

$$\omega_g = \frac{\kappa_S}{\tau_p} S_0 + \frac{n_{sp}}{S_0 \tau_p}. \tag{2.23}$$

With equations (2.11),(2.14),(2.22), it is possible to calculate the required injection current for a given frequency or intensity modulation of a laser. In Chapter 5, these equations will be used to generate a predistorted small signal to mitigate the chromatic dispersion.

In Figure 2.3 a optical eye diagram (2.3a) and the corresponding optical power and frequency modulation (2.3b) of the laser used throughout this work is shown. The laser bias current is $I_{bias} = 32\,\mathrm{mA}$ and the laser modulation current is $I_{mod} = 19\,\mathrm{mA}$. In Figure 2.2a it can be seen, that the laser bandwidth at this bias current I_{bias} is about 8 GHz. Due to the high modulation current and thus the low level of the current for the a *zero* bit (which is near laser threshold current $I_{th} \approx 10.6\,\mathrm{mA}$), the eye diagram of the laser signal shows significant overshoots.

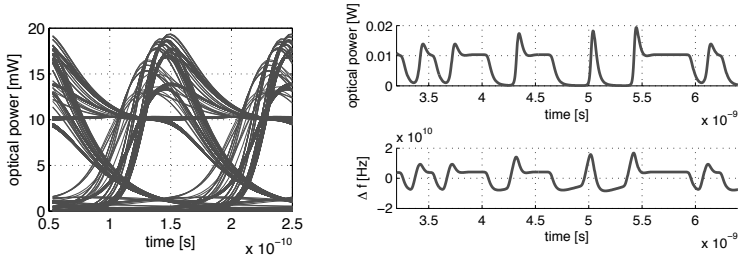

(a) optical eye

(b) optical power and frequency

Figure 2.3.: Typical signal of the used directly modulated laser,with $I_{bias} = 32\,\mathrm{mA}$ and $I_{mod} = 19\,\mathrm{mA}$.

CHAPTER 3

TRANSMISSION IMPAIRMENTS IN OPTICAL FIBERS

3.1. Overview

In this Chapter, optical fibers and the signal propagation in optical fibers are reviewed. In particular, the linear effect of the chromatic dispersion is explained, as it is the purpose of this work to present a technique to compensate it. Nonlinear effects are only briefly introduced, as there are less important for single wavelength system with transmission distances of about 100 km to 300 km.

The simplest optical fiber consists of a cylindrical core of silica glass with a refractive index n_1 and a surrounding cladding with a lower refractive index n_2 than the core (Figure 3.1). This type of fiber is called step–index fiber. With appropriate values for n_1 and n_2 with respect to the core diameter a the fiber supports only one mode and is called single mode fiber (SMF) [8]. Such fibers are typically used in optical transmission systems.

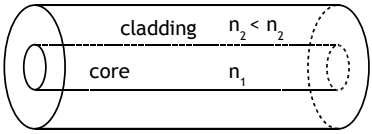

Figure 3.1.: Schematical drawing of a step–index fiber. Not true to scale.

3.2. Optical Losses

Fiber loss is one of the limiting factors in optical transmission systems. At least a minimum amount of power at the receiver is necessary to recover the signal. Changes in the average optical power P of a signal propagating inside a fiber, can be described with the following differential equation:

$$\frac{dP}{dz} = -\alpha_f P \tag{3.1}$$

where α_f is the attenuation coefficient of the fiber. With P_{in} being the launch power into the fiber the output power P_{out} at fiber length L is given as:

$$P_{out} = P_{in} \cdot e^{-\alpha_f L} \tag{3.2}$$

The fiber loss parameter is commonly expressed in units of dB/km:

$$\alpha_f[dB/km] = -\frac{10}{L}\log_{10}\left(\frac{P_{out}}{P_{in}}\right)[1/km] \approx 4.343 \cdot \alpha_f[1/km] \tag{3.3}$$

The fiber loss is typicaly caused by two processes: material absorption and Rayleigh scattering. The reason for material absorption are resonances of electrons or molecules induced by the incident light. For silica (SiO_2) the electronic resonance occurs at

wavelengths below $0.4\,\mu$m (ultraviolet light), whereas the molecular resonance occurs in the infrared region at wavelengths above $7\,\mu$m. But even if the commonly used wavelength in optical transmission systems is typically between $1.3\,\mu$m and $1.6\,\mu$m and therefore not in the mentioned regions of resonances, the resonance tails extend into the used wavelength region and attenuate the propagating light (see Figure 3.2). Beside these intrinsic absorption processes, there are also extrinsic absorption processes due to fiber impurities. In particular, the OH impurities result in a significant absorption at $1.39\,\mu$m. Recently so called *low water peak* fibers were introduced [9], where attenuation due to the resonance of the OH–ion is considerably reduced.

Rayleigh scattering is based on density fluctuation in fused silica. The resulting fluctuations in the refractive index cause light scattering in all directions. The fiber loss due to Rayleigh scattering is [10]:

$$\alpha_s = \frac{1}{\lambda^4} \cdot 0.7 \cdots 0.9 \,\frac{\mathrm{dB}}{\mathrm{km}} \mu\mathrm{m}^4 \tag{3.4}$$

depending on the constituents of the fiber.

3.3. Chromatic Dispersion

Based on the Maxwell equations, the propagation of light in an optical fiber may be written as [10]:

$$\nabla \times \nabla \times \vec{E} = -\frac{1}{c^2}\frac{\partial^2 \vec{E}}{\partial t^2} - \mu_0 \frac{\partial^2 \vec{P}}{\partial t^2} \tag{3.5}$$

where μ_0 is the vacuum permeability, $c = 1/\sqrt{\mu_0 \varepsilon_0}$ is the speed of light in vacuum and ε_0 is the vacuum permittivity, $\vec{E}$ is the electric field vector and $\vec{P}$ is the polarization induced by the electric field. In general, the polarization $\vec{P}$ is nonlinear in the electric field $\vec{E}$, but in a first step it is sufficient to consider a linear polarization

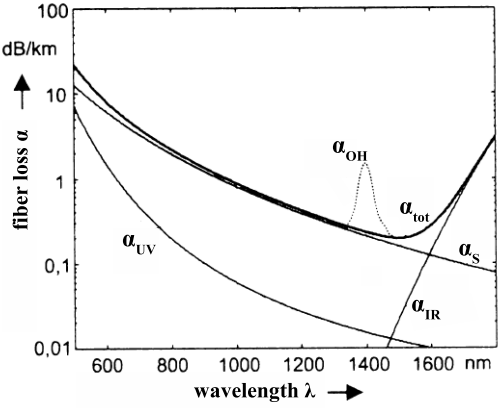

Figure 3.2.: Wavelength depending fiber loss (α_{UV} – ultraviolet absorption, α_{IR} – infrared absorption, α_s – Rayleigh scattering, α_{OH} – absorption due to OH impurities, α_{tot} – total fiber loss).

$\vec{P} = \vec{P}_L$:

$$\vec{P}_L(\vec{r}, t) = \varepsilon \int_{-\infty}^{\infty} \chi(t - t') \cdot \vec{E}(\vec{r}, t')\, dt', \tag{3.6}$$

with the linear susceptibility χ, which in general is a second–rank tensor that can be reduced to a scalar for an isotropic medium such as silica glass and a position vector $\vec{r}$. Now, the frequency dependent dielectric constant $\varepsilon(\omega)$ can be introduced:

$$\varepsilon(\omega) = 1 + \underline{\chi}(\omega), \tag{3.7}$$

where $\underline{\chi}(\omega)$ is the Fourier transform of $\chi(t)$. In general, $\varepsilon(\omega)$ is a complex value, where its real part is related to the refractive index n and its imaginary part is related to the absorption α. Due to

low optical losses in silica glass, $\varepsilon(\omega)$ can be assumed to be real, which means $\varepsilon(\omega) = n^2(\omega)$. In case of a step index fiber, which is commonly used for single mode fibers, the refractive index is independent of the spatial coordinates in both the core and the cladding of the fiber, respectively. Now, (3.5) and (3.6) can be written in the frequency domain:

$$\nabla^2 \underline{\vec{E}} + n_{1,2}(\omega)^2 k_0^2 \underline{\vec{E}} = 0. \tag{3.8}$$

with the free space wave number $k_0 = \omega/c = 2\pi/\lambda$, the vacuum wavelength λ and the refractive indices for the core and the cladding $n_{1,2}$, respectively. $\underline{\vec{E}}(\vec{r},\omega)$ is the Fourier transform of $\vec{E}(\vec{r},t)$, defined as:

$$\underline{\vec{E}}(\vec{r},\omega) = \int_{-\infty}^{\infty} \vec{E}(\vec{r},t)\exp(-j\omega t)dt. \tag{3.9}$$

For a weakly guiding fiber at single mode conditions, with a pulse spectrum $\Delta\omega$ that is assumed to be much narrower than the center frequency ω_0, i.e., $\Delta\omega \ll \omega_0$ the solution of (3.8) are two independent, orthogonal polarizations of $\vec{E}$:

$$\underline{\vec{E}}(\vec{r},\omega) = F(x,y)\underline{E}(0,\omega)\exp(-i\beta(\omega)z)\begin{pmatrix}\vec{e}_x \\ \vec{e}_x\end{pmatrix}. \tag{3.10}$$

Here, $F(x,y)$ describes the transversal distribution of the electrical field, which is independent of the spatial coordinate z. $E(0,t)$ is the initial field amplitude and $\beta(\omega)$ is the propagation constant. $\vec{e}_x$ and $\vec{e}_y$ are unit vectors in the x and y direction, respectively. It is common to express $\beta(\omega)$ with the Taylor series expansion around the carrier frequency, i.e. the frequency of the unmodulated light ω_0:

$$\beta(\omega) = \beta_0 + (\omega-\omega_0)\beta_1 + \frac{(\omega-\omega_0)^2}{2}\beta_2 + \frac{(\omega-\omega_0)^3}{6}\beta_3 + \cdots \tag{3.11}$$

with

$$\beta_m = \left(\frac{d^m\beta}{d\omega^m}\right)_{\omega=\omega_0} \tag{3.12}$$

where β_0 is a constant phase shift, $\beta_1 = 1/v_g = \tau$ is the inverse group velocity (or the group delay per length), β_2 is the group velocity dispersion (GVD) and β_3 is the dispersion slope. The change of the group velocity (described with β_2, β_3) leads to significant pulse distortions, which limits the maximum transmission distance in optical transmission systems. The common dispersion parameter D in units of ps/(km nm) is defined as:

$$D = \frac{d}{d\lambda}\left(\frac{1}{v_g}\right) = -\frac{2\pi c}{\lambda^2}\beta_2 \tag{3.13}$$

and consists of two parts, the material dispersion (D_M) and the waveguide dispersion (D_W):

$$D = D_M + D_W \tag{3.14}$$

The material dispersion occurs due to the frequency dependence of the refractive index $n(\omega)$ of silica. The origin of the frequency dependence is the same process as the one being responsible fiber attenuation [11, 10]: Characteristic resonance frequencies of the material at which the electromagnetic radiation is absorbed. With the Sellmeier equation the characteristic of the material dispersion can be expressed [10].

In contrast, the waveguide dispersion depends on the characteristic of the waveguide. Parameters like the core diameter, the difference of the refractive indices or the refractive index profile can significantly change the total dispersion D (see Figure 3.3). This means, depending on the fiber profile, it is possible to obtain a positive, negative or even a fiber with zero dispersion at a given wavelength. Also fibers with a flattened dispersion profile are designed having a constant dispersion over a relatively wide range from 1.3 to 1.6 μm [8].

To analyze the signal propagation in a dispersive fiber, it is common to separate the field of the slowly varying envelop $A(z,t)$ from the field $E(z,t)$:

$$E(z,t) = A(z,t)\exp\left(-j\beta_0 z + j\omega_0 t\right), \tag{3.15}$$

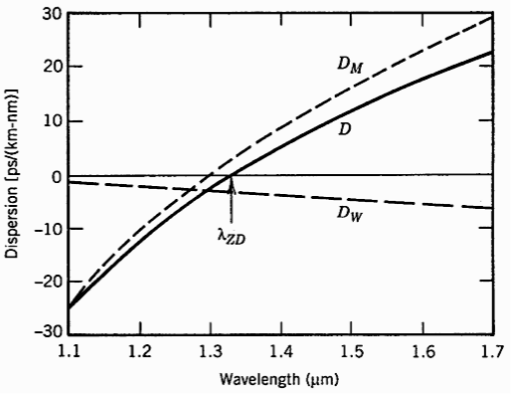

Figure 3.3.: Wavelength dependency of the total dispersion D and their relative contributors, material dispersion D_M and waveguide dispersion D_W for a standard single mode fiber. λ_{ZD} – zeros dispersion wavelength (from [8]).

Due to the fact that the group delay is mainly given by τz, the retarded time $T = t - \tau z$ can be introduced. Thus, with respect to $dT = dt$ and $\Delta\omega = \omega - \omega_0$, the Fourier transform of the amplitude $A(z,t)$ is:

$$\underline{A}(z,\Delta\omega) = \int_{-\infty}^{\infty} A(z, T+\tau z)\exp(-j\Delta\omega T)\, dT \tag{3.16}$$

$$= \exp(j\Delta\omega\, \tau z) \int_{-\infty}^{\infty} A(z,t)\exp(-j\Delta\omega t)\, dt \tag{3.17}$$

Because the lateral field distribution is independent of the spatial coordinate z, the one dimensional signal propagation inside a fiber

can be given by (compare (3.10) and (3.11)):

$$\underline{E}(z,\omega) = \underline{E}(0,\omega)\exp(-j\beta_0 z - j\beta_1\Delta\omega z - j/2\beta_2\Delta\omega^2 z). \quad (3.18)$$

Taking (3.15) and (3.18) and considering that $\underline{A}(0,\Delta\omega) = \underline{E}(0,\omega)$, (3.17) can be rewritten as:

$$\underline{A}(z,\Delta\omega) = \underline{A}(0,\Delta\omega)\exp(-\frac{j}{2}\beta_2\Delta\omega^2 z), \quad (3.19)$$

which is a solution of the following differential equation in the time domain:

$$\frac{\partial A(z,T)}{\partial z} = \frac{j}{2}\beta_2\frac{\partial^2 A(z,T)}{\partial T^2}. \quad (3.20)$$

Here, A is assumed to be normalized such that the optical power is $|A|^2$. This simple differential equation describes the pulse propagation in a dispersive fiber, taking only chromatic dispersion into account.

3.3.1. Chirped Gaussian Pulse

The broadening of a chirped pulse, and thus the transmission limit, depends on the chirp factor α and the chromatic dispersion β_2 of the transmission fiber. Based on the following analytical description of the pulse broadening of a Gaussian pulse, the maximum transmission distance of a directly modulated laser will be approximated. Additionally, different reported approaches to overcome the dispersion limit for a chirped signals will be discussed analytically.

An initial Gaussian pulse may be described as follows:

$$A(z=0,T) = \sqrt{P_0}\exp\left(-\frac{1}{2}\left(\frac{T}{T_0}\right)^2 + j\phi(T)\right), \quad (3.21)$$

where P_0 is the optical power and T_0 is the half–width of the optical power at the point $1/e$, which is related to the full–width half–maximum $T_{FWHM} = 2\sqrt{\ln(2)}\cdot T_0$.

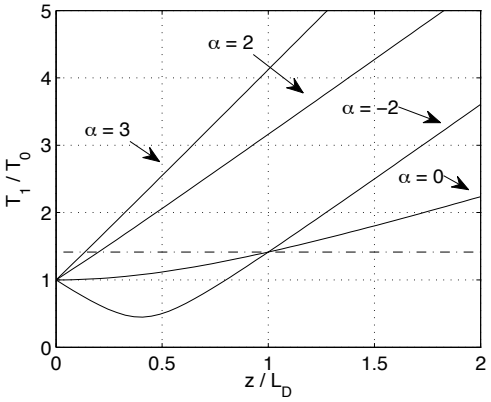

Figure 3.4.: Broadening of a chirped Gaussian pulse with $\beta_2 < 0$ (SSMF). A negative chirp $\alpha < 0$ results first in a narrower pulse shape that becomes broader after a specific transmission length. In case of a fiber with $\beta_2 > 0$, the same curves are obtained with a inverse sign of the chirp α.

Every intensity modulation of a directly modulated laser leads to a frequency modulation of the optical signal, as described in section 2.2. Considering only a transient chirp (see (2.20)), the phase modulation of the Gaussian pulse can be written as:

$$\phi(T) = -\frac{\alpha}{2}\left(\frac{T}{T_0}\right)^2 \tag{3.22}$$

Using (3.20), the pulse after transmitting over a fiber with the

length z can be described as [10]:

$$A(z,T) = \frac{A_0}{\sqrt{1+(\alpha-j)(\beta_2 z/T_0^2)}} \cdot \exp\left(-\frac{1+i\alpha}{2}\frac{T^2}{1+(\alpha-j)(\beta_2 z/T_0^2)}\right) \quad (3.23)$$

This means, the initial Gaussian pulse remains Gaussian, even with an initially modulated optical phase. Therefore, it is useful to describe the broadening of the pulse shape with respect to the initial pulse width T_0 [12]:

$$\frac{T_1}{T_0} = \sqrt{\left(1 \pm \alpha\frac{z}{L_D}\right)^2 + \left(\frac{z}{L_D}\right)^2} \quad (3.24)$$

with the half–width (at the power point 1/e) of the broadened pulse T_1 and the dispersion length $L_D = T_0^2/|\beta_2|$, where an initially unchirped pulse is broadened by the factor $\sqrt{2}$. The $\pm$ sign becomes positive if $\beta_2 < 0$ and negative if $\beta_2 > 0$.

In case of a 10 Gbit/s signal the full–width half–maximum at the transmitter may be $T_{FWHM} = 60$ ps and thus the dispersion length $L_D \approx 63$ km (with $D = 16\,\frac{\text{ps}}{\text{km nm}}$). The same pulse with chirp $\alpha = 2$ is already broadened by the factor $\sqrt{2}$ after $z = 0.2 \cdot L_D \approx 13$ km. This means that the maximum transmission length for the directly modulated laser signal is 5 times shorter than for an unchirped signal. In practice a directly modulated laser does not generate a Gaussian pulse and the frequency modulation consists not only of a transient chirp, but the analysis is still a good approximation of the possible transmission length of a chirped signal as it will be shown in section 4.1.

The behavior of a signal with a negative chirp ($\alpha < 0$), which can not be generated with a directly modulated laser, is quite different. As shown in Figure 3.4, a pulse with a chirp $\alpha = -2$ first becomes narrower before it broadens. After a transmission length $z = L_D$, it is broadened to the same width as an unchirped pulse.

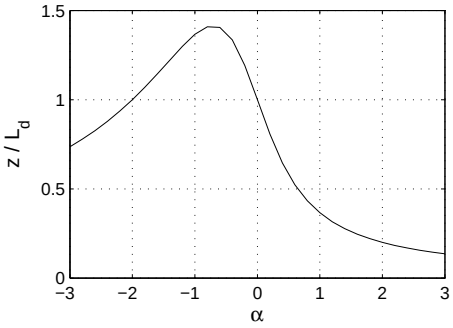

Figure 3.5.: The curve shows the relative transmission length z/L_D, at which the signal is broadened by a factor $\sqrt{2}$ as a function of chirp α for $\beta_2 < 0$. For $\beta_2 > 0$ the curve is mirrored at $\alpha = 0$.

In Figure 3.5 it is shown that a pulse with a chirp $\alpha \approx -0.7$ can improve the maximum transmission length by a factor 1.4 compared to an unchirped pulse. Because the chirp of a directly modulated laser is always positive, other modulators [13] or modulation techniques have to be used [14, 15] to improve the dispersion limited transmission length with a standard single mode fiber (SSMF) where $\beta_2 < 0$.

As can be seen in (3.24), if $\beta_2 > 0$ and the chirp $\alpha < 0$ the behavior of a Gaussian pulse is the same as with $\beta_2 < 0$ and $\alpha > 0$. Thus, using fibers like Cornings MetroCore with a dispersion $\beta_2 > 0$ leads to much larger transmission distances even for directly modulated laser signals at a wavelength of 1550 nm [16, 17, 18].

3.4. Kerr Effect

The main subject of this work is the precompensation of chromatic dispersion. But to study the behavior of a predistorted signal in

a typical transmission system, the impact of fiber nonlinearities will be considered in section 5.3.4. Therefore, the Kerr effect will be briefly introduced.

In section 3.3 the polarization $\vec{P}$ was assumed to be linear. In reality, all materials show a nonlinear behavior at high power densities. It is common to define a nonlinear refraction index $n'_{1,2}$ for the core and the cladding, respectively[10]:

$$n'_{1,2} = n_{1,2} + \overline{n}_2(P/A_{eff}). \tag{3.25}$$

Here, $n_{1,2}$ represents the linear part and $\overline{n}_2$ the nonlinear part of the refractive index, A_{eff} is the effective mode area and P is the optical power. In fact, the nonlinearity in silica is relatively small, but due to the high power density in the fiber and the long fiber length, the Kerr effect becomes relatively important for optical transmission systems. A very common description of the nonlinearities in optical fibers is the nonlinear Schrödinger equation [10]:

$$\frac{\partial A(z,T)}{\partial z} = j\frac{\beta_2}{2}\frac{\partial^2 A(z,T)}{\partial T^2} - \frac{\alpha_f}{2}A(z,T) - j\gamma|A(z,T)|^2 A(z,T) \tag{3.26}$$

with the nonlinear coefficient γ:

$$\gamma = \frac{\overline{n}_2\omega_0}{cA_{eff}} \tag{3.27}$$

The nonlinear Schrödinger equation (3.27) also includes the effect of chromatic dispersion as described in (3.20). Due to fiber loss, the optical power of a signal decreases while propagating in a fiber and thus the nonlinear effect becomes less important with increasing propagating length. Hence, it is useful to introduce the

effective length L_{eff}

$$L_{eff} = \int_0^L \exp(-\alpha_f z) dz \tag{3.28}$$

$$= \frac{1 - \exp(-\alpha_f L)}{\alpha_f}, \tag{3.29}$$

after which the influence of the nonlinearity of the signal can be neglected. The Kerr effects can be divided mainly into three parts:

- Self Phase Modulation (SPM),
- Cross Phase Modulation (XPM) and
- Four Wave Mixing (FWM).

While XPM and FWM are mainly mportant for long–haul wavelength division multiplexing (WDM) systems, SPM influences also single channel systems and thus, it will be discussed briefly.

3.4.1. Self Phase Modulation

Unlike the chromatic dispersion, SPM itself only changes the phase of the signal and not the pulse shape. The propagation constant becomes power dependent and can be written as:

$$\beta' = \beta + \frac{k_0 \overline{n}_2}{A_{eff}} |A|^2 = \beta + \gamma |A|^2. \tag{3.30}$$

The induced phase shift may be written as:

$$\Delta\phi_{SPM} = \int_0^L (\beta' - \beta)\, dz = \int_0^L \gamma P_{in} \exp(-\alpha z) dz = \gamma P_{in} L_{eff}. \tag{3.31}$$

This means, any variation of the optical power in time leads to a phase modulation and thus a frequency modulation as shown in

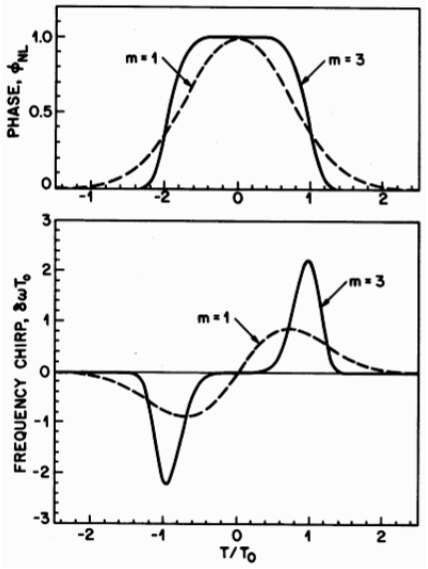

Figure 3.6.: Phase shift $\phi_{NL} = \phi_{SPM}$ induced by SPM and the resulting frequency modulation $\delta\omega$ for a Gaussian (dashed line) and a super–Gaussian pulse (solid line) (from [10]).

Figure 3.6. In presence of dispersion, the SPM induced phase shift leads to FM–AM conversion[1] and thus influences the transmission behavior of a transmission signal.

[1] frequency modulation – amplitude modulation conversion

CHAPTER 4

MODULATION FORMATS FOR DIRECTLY MODULATED LASERS

Before different approaches are studied in Chapter 5 to predistort the chromatic dispersion, different modulation techniques for a directly modulated laser are presented. The purpose is to compare already known modulation techniques for a directly modulated laser in terms of maximum achievable transmission distance and complexity. In Chapter 5, these modulation techniques will also be compared to the precompensation technique that will be introduced later.

Using a directly modulated laser is the easiest way to imprint data on an optical carrier. Here, the data is modulated onto the laser injection current and the resulting modulation format is a binary intensity modulation, also called On–Off–Keying (OOK). Directly modulated lasers at 1550 nm are widespread for optical transmission systems with data rates up to OC–48 (2.488 Gbit/s), as they meet the demands for a low cost system. However, taking the step to higher data rates like OC–192 (9.953 Gbit/s), the chirp induced by the directly modulated laser makes it more difficult to

achieve high transmission distances. Therefore different modulation techniques are reported for 10 Gbit/s directly modulated laser systems.

4.1. Non Return–to–Zero

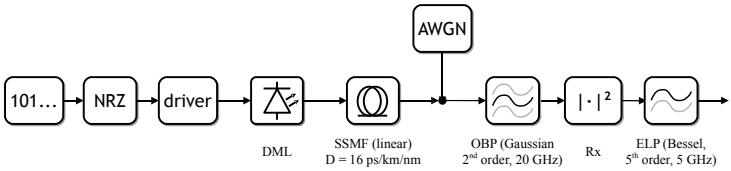

Figure 4.1.: Simulation setup for a directly modulated laser transmission system. For the used laser parameters see Appendix A.

The most common OOK modulation format for directly modulated laser is the non–return–to–zero (NRZ) modulation format. Here, a binary bit–sequence of "0" and "1" is directly imprinted in the optical intensity whereas between two adjacent "1" the signal does not return to zero level as with the return–to–zero (RZ) format[19].

The simulation setup used to study the system behavior of the NRZ format is schematically shown in Figure 4.1. The laser driver (and a bias–T) adds a modulation I_{mod} and a bias I_{bias} current to the NRZ modulated binary bit sequence to obtain a laser injection current. The bit sequence is a de Bruijn bit sequence with 2^{10} bit [20]. The modulated optical signal, generated by the laser, is then transmitted over a linear SSMF (nonlinearities of the fiber are neglected) with a dispersion parameter $D = 16\,\mathrm{ps/(km\,nm)}$. In order to calculate the bit error ratio (BER) for a given optical signal to noise ratio (OSNR), white Gaussian noise is added

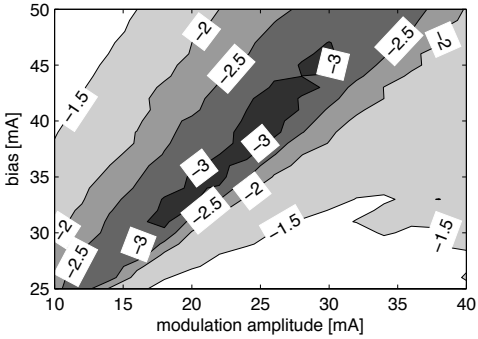

Figure 4.2.: Contour plot of the (logarithmic) BER for different bias and modulation (amplitude) currents of the laser injection current with a laser chirp $\alpha = 2$ (OSNR = 12 dB) in a back–to–back transmission scenario.

(AWGN) to the transmitted optical signal. The receiver consists of an optical 2^{nd} order Gaussian bandpass (OBP) with a bandwidth of 20 GHz, an ideal photodiode and an electrical 5^{th} order Bessel lowpass (ELP) with a cut–off frequency of 5 GHz. The maximum of the transfer function of the OBP matches with the center frequency of the unmodulated (CW) laser signal. The BER at the receiver is calculated using the Monte Carlo method with at least 40 counted errors. In principle, this setup is used for any simulation throughout this work with only a varying laser chirp parameter α.

As described in Chapter 2, the modulation characteristics and thus the BER for a given ONSR of the laser depend on the mean injection current. Figure 4.2 shows the dependence of the BER of the laser signal (back–to–back) from the bias I_{bias} and the mod-

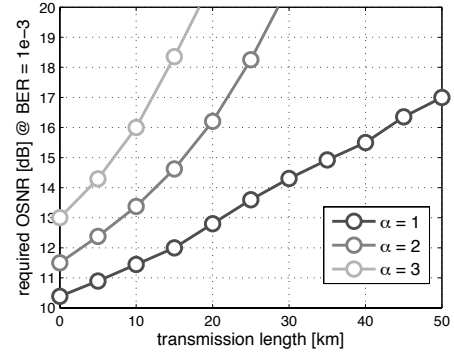

(a) Required OSNR as a function of the transmission length.

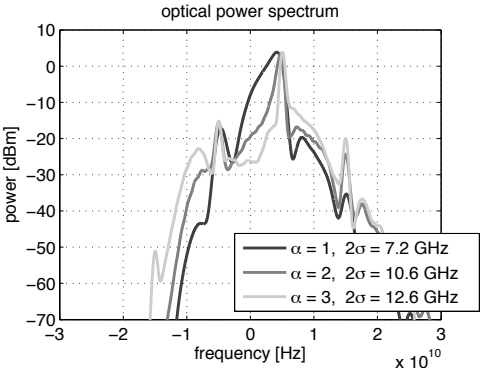

(b) Optical power spectrum and spectral width.

Figure 4.3.: Transmission behavior and optical power spectrum of an NRZ signal. The bias and modulation current are optimized for each laser chirp α for the back–to–back signal .

ulation current I_{mod}. The laser parameters that are used for the results in Figure 4.2 can be found in Appendix A and are used throughout this work with only a varying chirp parameter α (here $\alpha = 2$). The results show, that the bias and modulation current have to be optimized (e.g. in a brute force manner) even for a back–to–back transmission in order to obtain an optimal BER.

Additionally, the maximum transmission length of a directly modulated laser signal is limited by the laser chirp (see section 3.3.1), and thus by the width of the optical spectrum. This means for a NRZ modulated signal: The larger the laser chirp α, the shorter the maximum transmission length of the signal. In Figure 4.3 the transmission behavior and the optical power spectrum of three laser signals with different chirp factors $\alpha = 1, 2, 3$ are shown. The bias and modulation current of the signals are optimized for the BER of the back–to–back signal and are shown in table 4.1.

chirp α	bias [mA]	modulation [mA]
1	43	30
2	32	19
3	31	16

Table 4.1.: Optimized bias and modulation currents (amplitude) of the laser driver for the back–to–back signal of different laser chirps

As can be seen in Figure 4.3a, the maximum transmission length (with a required OSNR $\approx 20\,\mathrm{dB}$) for a typical laser laser chirp of $\alpha = 2 \cdots 3$ is between 20 km and 30 km. The corresponding optical power spectra are shown in Figure 4.3b. Depending on the chirp factor α, the spectral width is between 7.2 GHz for $\alpha = 1$ and 12.6 GHz for $\alpha = 3$. The spectral width is defined as the two sided standard deviation (2σ) of the optical spectrum. The difference in

the required OSNR for the back–to–back signal results from the relatively small optical band–pass that is used for the simulations. While the waveform of the low chirp signals ($\alpha \leq 1$) stays almost unchanged, the signals with a high chirp change due to a wider optical spectrum.

An even more restricted experimental result for the maximum transmission distance is published by Morton et al. [21]. Using a low chirp directly modulated laser ($\alpha \approx 1$), an error free transmission over 18.5 km SSMF was shown. In order to reduce the laser induced signal chirp, and thus to narrow the optical spectrum, it is reasonable to increase the laser bias current. As Mohrdiek et al. [22] have shown, a prior back–to-back optimized laser signal can enhance the maximal transmission distance by a factor of four if the bias and the modulation current is adapted.

4.2. Dispersion Supported Transmission

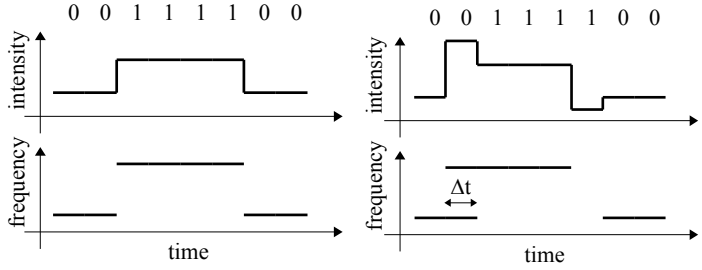

(a) Laser signal (b) Signal after dispersive fiber

Figure 4.4.: Principle of dispersion supported transmission

To overcome the dispersion limit for directly modulated lasers Wedding et al. [23, 1] proposed the dispersion supported transmis-

transmission distance [km]	bias [mA]	modulation [mA]	low pass filter bandwidth [GHz]
50	52	24	4
120	48	18	2
200	37	14	2
240	34	13	2

Table 4.2.: Optimized bias and modulation (amplitude) currents of the laser driver and low pass filter bandwidth for the dispersion supported transmission for different transmission distances. Laser chirp $\alpha = 2$.

sion (DST). The main concept of the dispersion supported transmission is the conversion of the laser induced frequency modulation into an amplitude modulation of the signal by the dispersion of the transmission fiber.

The concept is shown in Figure 4.4. Assuming only an adiabatic chirp, the pulse shape of the frequency modulation is the same as the amplitude modulation. This means the pulse shape of the “1” symbol has a higher amplitude with a higher frequency than the pulse shape of the “0” symbol (Figure 4.4a). Because of chromatic dispersion in the transmission fiber and the chirp of the signal, the corresponding pulse shape for the “1” symbol is propagating faster inside the fiber than the “0” pulse shape (Figure 4.4b). Thus the initially NRZ modulated signal becomes a differential signal, which needs an integrator to be demodulated. After direct detection of the signal, a first order low–pass filter as an integrator and a decision unit are used to recover the original data signal. Depending on the laser parameters such as the chirp, and the transmission distance, the operating point (i.e. laser bias and modulation current) and the electrical receiver filter have to be optimized. This means, transmitter and receiver have to be adjusted for every transmission distance.

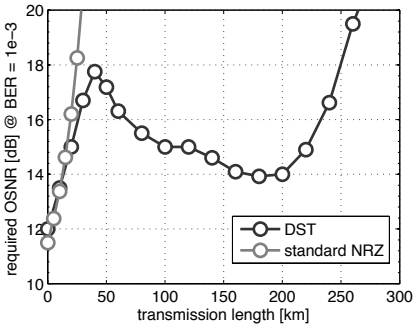

Figure 4.5.: The dispersion supported transmission expands the dispersion limited transmission length by a factor of ten. The chirp factor is $\alpha = 2$ and nonlinear effects are neglected.

The system parameters used to numerically analyze the dispersion supported transmission are the same as in section 4.1. The only difference is the first order electrical low–pass filter at the receiver. The chirp factor is $\alpha = 2$ and fiber nonlinearities are neglected. The optimized bias and modulation currents and the bandwidth of the low pass filter are given in table 4.2 for different transmission distances.

The simulation results in figure 4.5 show that the dispersion supported transmission expands the transmission limit by a factor of ten, compared to the back–to–back optimized standard NRZ modulation. In the range from 0 km to about 40 km, the dispersion supported transmission shows a similar system performance as a standard NRZ directly modulated laser signal. In the range from 40 km to about 200 km, the FM–AM conversion, induced by the chromatic dispersion of the transmission fiber, leads to a decrease of the required OSNR. After 200 km transmission distance, the

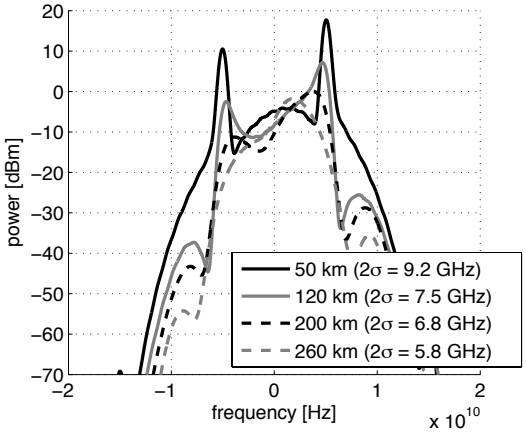

Figure 4.6.: Optical power spectrum of different DST signals.

required OSNR increases again. The range behind 40 km is called the dispersion supported transmission range [23].

Figure 4.6 shows the optical power spectrum of different dispersion supported transmission signals. The spectral width (2σ) of the dispersion supported transmission signal for 50 km is about the same as for the NRZ signal (see section 4.1). With growing transmission distance, the spectral width of dispersion supported transmission signals becomes narrower. For 260 km transmission distance, the spectral width of the dispersion supported transmission signal is only about 5.8 GHz, which leads to a much higher dispersion tolerance. This means that the enhanced transmission distance of the dispersion supported transmission may also be explained by the narrow optical power spectrum of optimized dispersion supported transmission signals.

In addition to the binary dispersion supported transmission format, also multi–level dispersion supported transmission formats for data rates of 20 Gbit/s and 40 Gbit/s are published [24, 25].

In comparison to the standard NRZ modulation, the dispersion supported transmission significantly extends the transmission length of a directly modulated laser without additional optical or electrical components[1], but with the disadvantage of having to adjust the transmitter and the receiver for every different transmission distance.

4.3. Chirp Managed Laser

Another approach to enhance the transmission distance of directly modulated lasers is the commercially available chirp managed laser (CML) [2, 26]. The dispersion tolerance of the CML results mainly from a high extinction ratio and a relative narrow optical spectrum.

Due to the distinct frequencies of the "0" and the "1" bit waveform of a directly modulated laser, the laser signal is filtered by the edge of an optical filter or optical spectrum reshaper (OSR) (figure 4.7), such that the energy of a "0" bit is reduced and thus the extinction ratio of the signal is increased. Compared to a common directly modulated laser signal, the extinction can be significantly increased, even if the laser is driven high above threshold with a low modulation current. This also means that the bias and modulation current of the laser can be assigned in a way such that the frequency modulation between a "0" and a "1" bit is about 5 GHz and is dominated by adiabatic chirp. In case of a 100 ps bit length (i.e. 10 Gbit/s data rate) the phase shift of two "1" bits separated by an odd number of "0" bit is then:

$$\Delta\phi_{101} = \Delta\omega_{101} t = 2\pi \cdot 5\,\mathrm{GHz} \cdot 100\,\mathrm{ps} = \pi. \tag{4.1}$$

Thus, the obtained modulation format is line–coded and it is very similar to the optical duobinary (DB) modulation format [27]. In presence of chromatic dispersion, the energy of the "1" bits is spread into adjacent "0" bits and would normally close the eye.

[1] The electrical low pass may be realized with a different biased photodiode

But due to the destructive interference of the "1" bits separated by an odd number of "0" bits, the eye remains open and can be easily detected. Additionally, the chirp managed laser signal has a suppressed carrier and the optical power spectrum has only half the bandwidth of the standard externally modulated NRZ modulation format [28]. A transmission distance of up to 250 km (4200 ps/nm) without dispersion compensation at 10 Gbits with 4,8 dB penalty is published by Mahgerefteh [2].

As shown in figure 4.8, the chirp managed laser has a similar dispersion tolerance like the dispersion supported transmission. Additionally, the chirp managed laser is applicable to a transmission system without adjusting the transmitter and the receiver for different transmission distances. But in contrast to the dispersion supported transmission the chirp managed laser requires an optical filter to reshape the complex waveform of the laser, which makes the concept more complex.

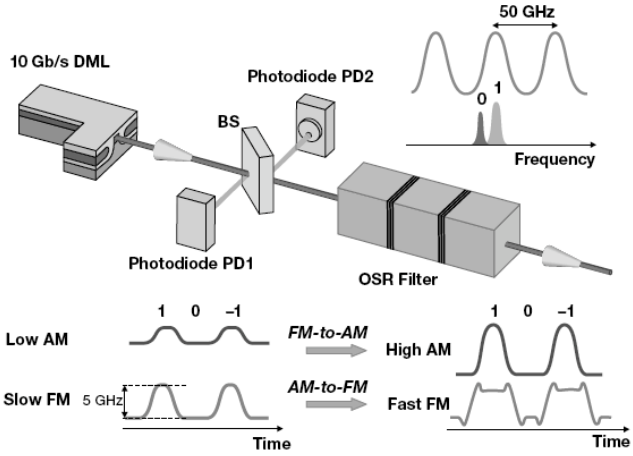

Figure 4.7.: Principle of operation of a chirp managed laser (from [26]).

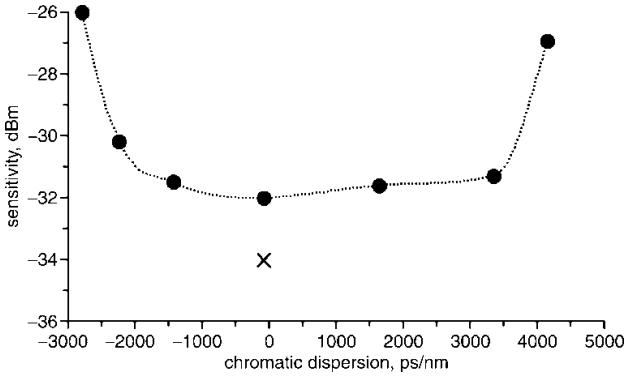

Figure 4.8.: Sensitivity penalty against fiber dispersion of a chirp managed laser (from [2]).

CHAPTER 5

ELECTRONIC PREDISTORTION CONCEPTS

The standard technique to compensate the effect of chromatic dispersion is the usege of dispersion compensating fibers (DCF). These DCFs have a negative dispersion parameter D (i.e. $\beta_2 > 0$) and thus, the DCF is able to compensates the dispersion, accumulated by transmission over fibers with positive dispersion (i.e. $\beta_2 < 0$) such as a SSMF.

The approach in this work deals with replacing the inline DCF with electronic signal processing in the transmitter. Due to the fact that the chromatic dispersion is a linear operation on the optical field, it is possible to calculate a predistorted complex optical field $\underline{A}_{in}$ that compensates the chromatic dispersion for a certain transmission length L and a given target signal $\underline{A}_{out}$ (i.e. complex optical field). Using (3.20), the predistorted signal $\underline{A}_{in}(L, \Delta\omega)$ is:

$$\underline{A}_{in}(L, \Delta\omega) = \underline{A}_{out}(\Delta\omega) \exp(+\frac{j}{2}\beta_2 \Delta\omega^2 L), \tag{5.1}$$

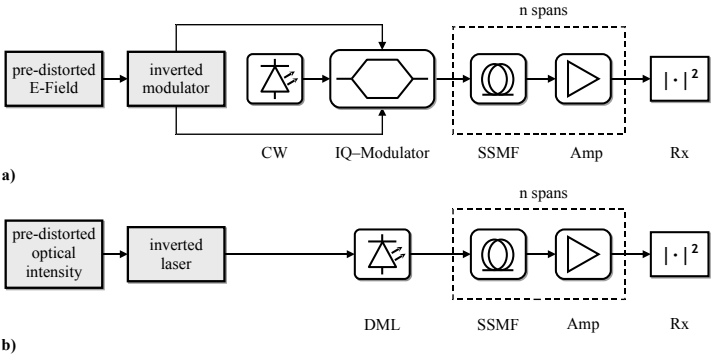

Figure 5.1.: Principle of signal predistortion for a vector modulator (a) and a directly modulated laser (b).

This means that by using a vector modulator, which modulates the complex optical field $\underline{A}_{in}$, any amount of dispersion can be predistorted and thus very large transmission distances can be obtained without inline compensation [4, 29]. McGhan et al. published a transmission at 10 Gbit/s with a dual parallel Mach–Zehnder modulator over 5120 km SSMF (ITU–T G.652) at the OFC[1] 2005 [29]. Systems with electronic predistortion are also commercially available. Here the maximum transmission length at 10 Gbit/s is more than 2000 km SSMF [30].

With respect to signal predistortion, the difference of between a directly modulated laser system and a transmission system with a vector modulator is schematically drawn in Figure 5.1. Due to the fact that a directly modulated laser cannot independently modulate both the optical intensity and the optical phase (and thus the complex optical field), the analytically estimated predistorted signal from (5.1) *cannot* be generated by a directly modulated

laser.

However, for direct detection systems, the information of the optical phase at the receiver is irrelevant and can therefore be used as a degree of freedom to deal with the phase dependence of the intensity at the laser. The purpose is now to obtain the predistorted intensity at the fiber input for a given target format of the optical intensity and a specified relation of the intensity and phase at the transmitter (e.g. the chirp). Once this predistorted signal is estimated, the nonlinear behavior of the laser has to be considered to obtain the corresponding laser injection current.

In this work different approaches are studied to obtain a signal predistortion for a directly modulated laser system. Based on a small signal approach, it is possible to calculate a predistorted laser injection current analytically for signals with a small extinction ratio. Due to the restriction of the small signal approach also two large signal approaches are studied. Linear and nonlinear finite impulse response (FIR) filters will be used to prefilter the laser injection current according to a desired target modulation format. In addition, an artificial neural network is used to estimate a laser injection current that leads to an optimum BER after transmission.

5.1. Small Signal Approximation

In case of a small signal approximation a fiber transfer function for the optical power and the optical phase can be obtained. With that fiber transfer function it is possible to analytically calculate the predistorted, dispersion compensating signal for a directly modulated laser.

Considering the slowly varying envelope of the optical field

$$A(t) = \sqrt{P(t)}\exp(j\phi(t) + j\omega_0 t) \tag{5.2}$$

[1]Optical Fiber Conference

with the optical power $P(t)$, the optical phase $\phi(t)$ and the angular carrier frequency ω_0, the signal degradation due to chromatic dispersion can be described in the frequency domain for the optical intensity and the optical phase with a transfer matrix [31] :

$$\begin{pmatrix} \frac{\Delta P_{out}(j\omega)}{2P_0} \\ \phi_{out}(j\omega) \end{pmatrix} = \begin{pmatrix} \cos(\omega^2 F) & -\sin(\omega^2 F) \\ \sin(\omega^2 F) & \cos(\omega^2 F) \end{pmatrix} \cdot \begin{pmatrix} \frac{\Delta P_{in}(j\omega)}{2P_0} \\ \phi_{in}(j\omega) \end{pmatrix} \tag{5.3}$$

where $P_{in/out} = \Delta P_{in/out} + P_0$, $\Delta P_{in/out} \ll P_0$ is the small signal approximation for the intensity at the fiber input and the fiber output, respectively. ω is the angular frequency and $F = \beta_2 L/2$ is a dispersion parameter with L being the transmission distance. In order to calculate a predistorted signal (i.e. to invert (5.3)), a negative fiber length L has to be assumed. The relation between P_{in} and ϕ_{in} is given by the laser parameters and is also called the phase–to–intensity ratio PIR_0 of the laser. The PIR changes because of the chromatic dispersion with the transmission length and can be expressed as:

$$\mathrm{PIR}(L) = \frac{\phi_{out}}{\Delta P_{out}/P_0} \tag{5.4}$$

$$= \frac{\frac{\Delta P_{in}}{(2P_0)} \sin(\omega^2 F) + \phi_{in} \cos(\omega^2 F)}{\frac{\Delta P_{in}}{(P_0)} \cos(\omega^2 F) - 2\phi_{in} \sin(\omega^2 F)} \tag{5.5}$$

$$= \frac{\frac{1}{2} \sin(\omega^2 F) + \mathrm{PIR}_0 \cos(\omega^2 F)}{\cos(\omega^2 F) - 2\ \mathrm{PIR}_0 \sin(\omega^2 F)} \tag{5.6}$$

with the initial PIR at the fiber input (see (2.22)):

$$\mathrm{PIR}_0 = \frac{\phi_{in}}{\Delta P_{in}/P_0}. \tag{5.7}$$

Together with (5.3), the predistorted optical power ΔP_{in} may be written as:

$$\Delta P_{in}(j\omega) = \Delta P_{out}(j\omega) \frac{1}{H_f^{(e)}(L, j\omega)} \tag{5.8}$$

with the fiber transfer function for the optical power:

$$H_f^{(e)}(L, j\omega) = \frac{1}{\cos(\omega^2 F) + 2\mathrm{PIR}(L)\sin(\omega^2 F)}. \tag{5.9}$$

It should be noted, that the fiber transfer function for the optical power $H_f^{(e)}$ is related to the phase–to–intensity ratio PIR of the laser and thus to the mean value of the optical power P_0. In order to obtain the required laser driver current ΔI_{in} for the predistorted intensity, the laser transfer function for the optical power $H'_{LD}(j\omega)$ (compare (2.16)) may be used:

$$\Delta I_{in}(j\omega) = \frac{e}{\tau_{ph}} \frac{1}{H'_{LD}(j\omega)} \frac{1}{H_f^{(e)}(L, j\omega)} \Delta P_{out}. \tag{5.10}$$

Analyzing the capability of the small signal approximation to predistort the chromatic dispersion, the predistorted injection current ΔI_{in} is used to modulate a rate equation based laser model as in Figure 5.2. The bias and modulation intensity of the target format P_{out} (i.e. the desired signal after transmission) is optimized for every transmission distance to fulfill the requirements of the small signal approximation. The performance of the signal predistortion is given in terms of the extinction ratio after transmission, as it is the aim to proof the possibility to predistort the chromatic dispersion with a directly modulated laser. Thus no noise is added to the signal.

The numerical results in Figure 5.3 show that the optical eye diagram remains open after up to 2000 km transmission (SSMF). The inset in Figure 5.3 shows the optical eye after 2000 km fiber transmission. This means that it is theoretically possible to calculate a dispersion precompensating laser signal, but only in case of signals with a very low extinction ratio. For practical systems a much higher extinction ratio after transmission is required, and thus a large signal approach has to be taken.

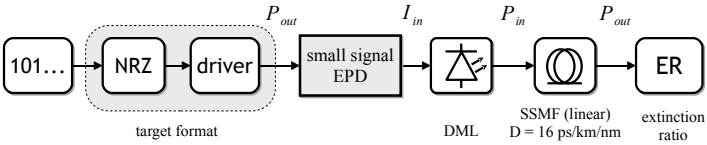

Figure 5.2.: Simulation setup for the small signal predistortion. The driver sets the bias and modulation intensity of the target format.

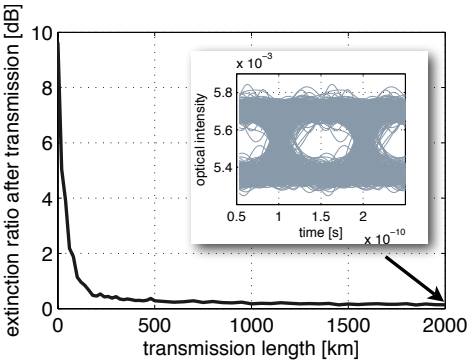

Figure 5.3.: Extinction ratio ($\mathrm{ER} = 10 \cdot \log\left(\frac{\min(P_1)}{\max(P_0)}\right)$) of the optical intensity after transmission, for the analytically predistorted signal using the small signal approximation. No optical or electrical filter are used at the receiver.

5.2. Finite Impulse Response Filter

The small signal approximation in Section 5.1 leads to a transfer function of the optical transmission system (i.e. the directly modulated laser and the optical fiber) for the optical power. Due to the restricted scope of this approach, the transfer function can not be used for a large signal. The Wiener filter theory [32] for FIR filters instead may be used to identify the impulse response of an unknown system (or the inverted unknown system) without the restriction of a small signal. Therefore, FIR filters as a simple and inherently stable class of filters [32] may be used to identify the system transfer function related to the laser injection current I_{in} and the target format P_{out} and thus to predistort the chromatic dispersion.

Considering a vector modulated transmission system, Said et al. [33] used two linear electrical FIR filters (for the inphase and quadrature component of the optical signal) as pre-filters for a duobinary modulated transmission system to precompensate the chromatic dispersion. Due to the fact that the fiber transfer function of the complex optical signal $H_f^{(o)}(z, j\omega) = \exp(-\frac{j}{2}\beta_2\Delta\omega^2 z)$ (see (3.18)) is linear, two linear FIR filters are capable to entirely predistort the chromatic dispersion of the fiber. Transmission distances up to 800 km without inline compensation are published.

In case of a directly modulated laser system, chromatic dispersion will be predistorted in the electrical domain. This means the optical signal is squared and the fiber transfer function related to the optical power is nonlinear and depends on the optical signal at the fiber input. Therefore, there are restrictions to the capability of an FIR filter to invert the transmission system and a nonlinear FIR filter will be introduced to estimate the fiber transfer function of the optical power.

Before the system behavior of FIR filters will be studied, in the following two sections linear and nonlinear FIR filters are introduced in more detail.

5.2.1. Linear FIR Filter

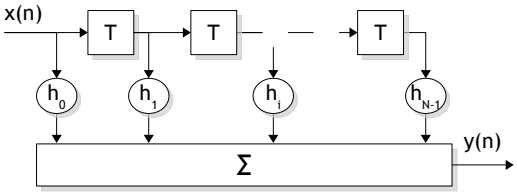

Figure 5.4.: Linear finite impulse response (FIR) filter with a time delay of T.

The following introduction to FIR filters is based on discrete–time signals in contrast to continuos–time signals used in previous chapters of this thesis. While a continuos–time signal is denoted as $y(t)$, a discrete–time signal is denoted as $y(n) \equiv y(nT)$, with $n \in \mathbb{Z}$ and T the sampling interval.

Linear FIR filters are defined with their filter coefficients h_i and the number of filter coefficients N. The output of the filter $y(n)$ may be described as a convolution between the filter input $x(n)$ and the filter coefficients, as indicated schematically in Figure 5.4:

$$y(n) = \sum_{i=0}^{N-1} h_i \cdot x(n-i) \tag{5.11}$$

As the coefficients h_i describe the impulse response of the FIR filter, it is the purpose to find coefficients which represent the impulse response of the inverted optical transmission system. Before the FIR filter will be used to predistort the signal, the Wiener theory will be shortly introduced where the filter is used as an post–filter after the system (Figure 5.5).

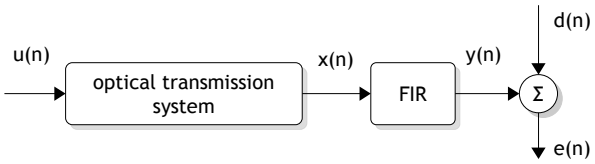

Figure 5.5.: Block diagram of the filtering problem. Typically the filter should invert the optical transmission system, which means: $u(n) = d(n)$ (ignoring any time delays of the system or the filter).

The filtering problem regarding to Figure 5.5 may be depicted as follows: Minimizing the summed mean–square error $e^2(n) = (d(n) - y(n))^2$:

$$J(h) = \sum_{n=-\infty}^{\infty} e^2(n) = \sum_{n=-\infty}^{\infty} (d(n) - y(n))^2 \tag{5.12}$$

where the desired signal $d(n)$ may be the uncorrupted input signal of the transmission system or the target signal after transmission. Often $d(n)$ is called the training signal of the filter. $y(n)$ is the filter output and corresponding to Figure 5.5 the equalized signal after transmission. This also means that signal degradations due to the laser modulation may be compensated as well. In order to minimize the error function J, it is appropriate to define a gradient vector, where the i–th element is the partial derivative with respect to h_i:

$$\nabla_i = \frac{\partial}{\partial h_i}. \tag{5.13}$$

To minimize the error function $\min(J)$ means:

$$\nabla_i J(h) = 0 \qquad \text{for } i = 0, 1 \cdots N-1 \tag{5.14}$$

$$\tag{5.15}$$

and thus:

$$\begin{aligned} 0 &= \sum_{n=-\infty}^{\infty} \frac{\partial e^2(n)}{\partial h_i} \\ &= -2 \sum_{n=-\infty}^{\infty} e(n) \frac{\partial y(n)}{\partial h_i} \\ &= \sum_{n=-\infty}^{\infty} e(n) x(n-i) \end{aligned} \tag{5.16}$$

Using $e(n) = d(n) - \sum_{k=0}^{N-1} h_k x(n-k)$, the equation (5.16) may be rewritten as follows:

$$\sum_{n=-\infty}^{\infty} \sum_{k=0}^{N-1} h_k x(n-k)\, x(n-i) = \sum_{n=-\infty}^{\infty} d(n) x(n-i) \qquad \text{for } i = 0, 1 \cdots N-1 \tag{5.17}$$

where the left and the right hand side of (5.17) are

- the autocorrelation function of the filter input: $r(k-i) = x(n-k)x(n-i)$ and
- the cross–correlation function between the filter input and the desired filter output: $p(-i) = d(n)d(n-i)$.

Equation (5.17) is know as the Wiener–Hopf equation [34]. Introducing the $N \times N$ autocorrelation matrix

$$\underline{R} = \sum_{n=-\infty}^{\infty} \vec{x}(n)\, \vec{x}^T(n) \tag{5.18}$$

with the vectorized filter input $\vec{x}(n) = [x(n-0), x(n-1), \cdots, x(n-N-1)]^T$, and the $N \times 1$ cross–correlation vector

$$\vec{p} = \sum_{n=-\infty}^{\infty} \vec{x}(n) d(n) \tag{5.19}$$

the Wiener–Hopf equation may be rewritten in the matrix form [34]:

$$\underline{R}\,\vec{h} = \vec{p} \tag{5.20}$$

with the filter coefficient vector $\vec{h} = [h_0, h_1, \cdots, h_{N-1}]^T$. To solve this equation, both sides of (5.20) may be multiplied by $\underline{R}^{-1}$:

$$\vec{h} = \underline{R}^{-1}\vec{p} \tag{5.21}$$

With (5.21), it is possible to estimate the coefficients $\vec{h}$ for an FIR filter that inverts the preceding optical transmission system (Figure 5.5) and thus equalizes the chromatic dispersion *after* fiber transmission. In section 5.2.3 this approach will be used to analyze the performance of FIR filters to equalize chromatic dispersion at the receiver. Thereafter, in section 5.2.4 an approach to use FIR filters to precompensate the chromatic dispersion at the transmitter will be introduced.

5.2.2. Nonlinear FIR filter (Volterrra Filter)

As already mentioned, the effect of chromatic dispersion in the electrical domain is nonlinear due to the square of the optical signal and thus, a linear FIR filter can compensate it only partially. The Volterra Filter, based on the Volterra series expansion, is a nonlinear FIR filter that is used in a relatively wide range of communication problems [35, 36, 37]. In optical communication systems, Xia et al. used a Volterra FFE–DFE filter for equalization of the received electrical signal [38].

The Volterra series expansion may be written as [39]:

$$\begin{aligned} y(n) = h_1^{(0)} &+ \sum_{m_1=0}^{\infty} h_{m_1}^{(1)}\, x(n-m_1) \\ &+ \sum_{m_1=0}^{\infty}\sum_{m_2=0}^{\infty} h_{m_1,m_2}^{(2)}\, x(n-m_1)x(n-m_2) \\ &+ \sum_{m_1=0}^{\infty}\sum_{m_2=0}^{\infty}\sum_{m_3=0}^{\infty} h_{m_1,m_2,m_2}^{(3)}\, x(n-m_1)x(n-m_2)x(n-m_3) \\ &+ \cdots \end{aligned} \tag{5.22}$$

As can be seen in (5.22), the Volterra series expansion combines the memory behavior of an ordinary FIR filter (second term) and the nonlinearity of the Taylor series expansion. The coefficients $h_{m_1,m_2,\cdots}^{(p)}$ are known as the Volterra kernel. The structure of the Volterra filter (based on a truncated Volterra series) is similar to a linear FIR filter, but with the difference of a multiplication of different delayed signals. Figure 5.6 shows a second order Volterra filter with two delay elements ($N = 2$). As can be seen, not all coefficients of (5.22) are represented, which is due to the symmetric behavior of coefficients of the Volterra series. However, the number of coefficients are growing with N^p, where N is the number of delay elements and p is the order of the truncated Volterra series.

As with an ordinary FIR filter, the vectorized Wiener-Hopf equation (5.21) can be used to derive the Volterra filter coefficients in an implementation like in Figure 5.5 [40]. For this purpose it

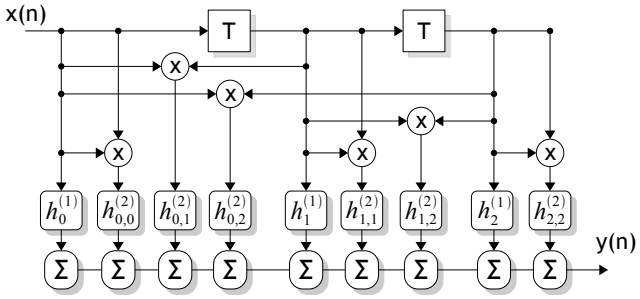

Figure 5.6.: Volterra filter of 2nd order with two delay elements an 9 filter coefficients.

is appropriate to write the filter coefficient vector as follows:

$$\begin{aligned}\vec{h} =&[h_0^{(1)}, h_1^{(1)}, \cdots, h_{N-1}^{(1)}, \\ &h_{0,0}^{(2)}, h_{0,1}^{(2)}, \cdots, h_{0,N-1}^{(2)}, \cdots, h_{N-1,N-1}^{(2)}, \\ &\vdots \\ &h_{N-1,\ldots}^{(p)}]^T\end{aligned} \tag{5.23}$$

while for the filter input vector $\vec{x}(n)$ the nonlinearity may be described:

$$\begin{aligned}\vec{x} =&[x(n-0), x(n-1), \cdots, x(n-1), \\ &x(n-0)x(n-0), \cdots, x(n-0)x(n-N-1), \cdots, x^2(n-N-1), \\ &\vdots \\ &x^p(n-N-1)]^T\end{aligned} \tag{5.24}$$

In this way, the autocorrelation matrix $\underline{R}$ (5.18) and the cross–correlation vector $\vec{p}$ (5.19) can be easily derived and thus the vectorized Wiener–Hopf equation may be solved to estimate the coefficients of a Volterra FIR filter.

5.2.3. Post–Filter

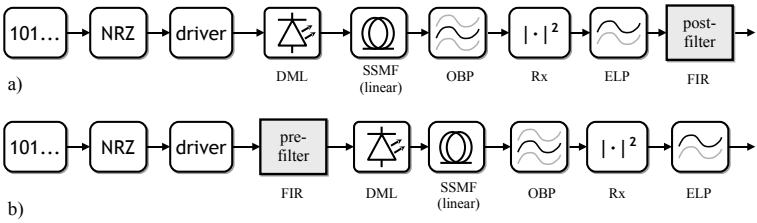

Figure 5.7.: Concept of a) pre- and b) post-filter.

The Wiener–Hopf equation makes it easy to equalize a transmission system at the receiver using a post–filter (see Figure 5.7), but it does not help to achieve the coefficients of a pre–filter. Thus, in a first step the ability to compensate signal distortions due to chromatic dispersion with a FIR post–filter will be analyzed. Then, in a second step, a technique to obtain a pre–filter will be introduced.

Figure 5.8 shows the simulated transmission system to obtain the coefficients of the post–filter. The purpose of that simulation setup is to equalize the chromatic dispersion of the fiber (Figure 5.8a) and the chromatic dispersion together with the nonlinearity of the laser (Figure 5.8b). That means in a first scenario the FIR filter is trained with the back to back signal of the directly modulated laser (Figure 5.8a) with a bias and modulation current of the laser as shown in Table 4.1 for a laser chirp $\alpha = 2$. In a second scenario the FIR filter is trained with an NRZ target format (Figure 5.8b) with a bias of 5.5 mW and a modulation amplitude of 4.5 mW. As a training sequence for both scenarios, a de Bruijn bit sequence of length of 2^{11} is used. The FIR filter is fractionally spaced, which means that the signal is sampled with 2 samples per bit. White Gaussian noise (AWGN) is added in the

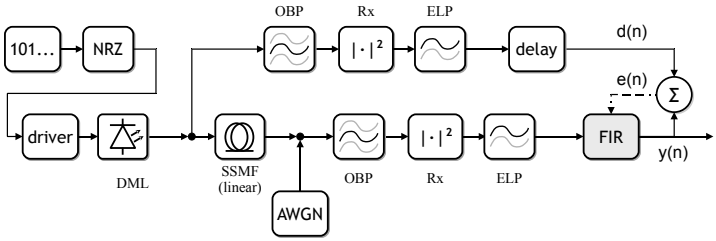

(a) directly modulated laser signal for training

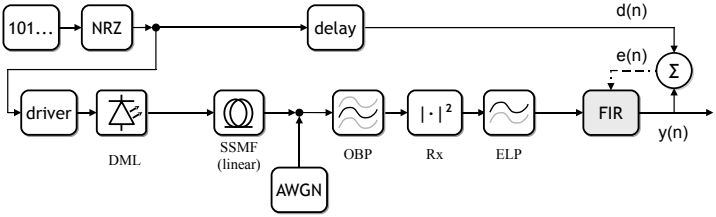

(b) NRZ signal for training

Figure 5.8.: Simulation setup for estimating the coefficients of a post-filter for a directly modulated laser system.

transmission path (fiber path). In a first simulation (*training run*) the filter coefficients for the actual setup (transmission length, different FIR configurations) will be obtained. Then, in a second simulation run (*performance evaluation*) the required OSNR for the post-equalized transmission system will be estimated. In the second simulation for the performance evaluation of the trained FIR filter, a different noise seed is used than in the training run. The delay–block in both setups may be set such that the FIR filter will considers not only passed samples for equalizing of a sample but also the samples in the "future". This is important, as a signal pulse spreads into both time directions due to chromatic dispersion. The optimum delay will be estimated by simulations with different delay values and depends on the transmission length

and the modulation format (e.g. DML or NRZ).

The system performance is shown in Figure 5.9 for different FIR Volterra filter orders including linear FIR filters[2]. As expected, with growing Volterra filter order, the achievable transmission length increases. For the DML target format the maximum transmission length for a linear filter (1^{st} order Volterra) is about 40 km (at 22 dB req. OSNR). This doubles using a 3^{rd} order Volterra filter. Compared to the not equalized system, this is a transmission enhancement of about 10 km and 50 km, respectively. Using an NRZ signal as the training signal, the maximum transmission length is between 50 km and 100 km. The different performance between the DML target format and the NRZ target format in the back–to–back case (≈ 2 dB) shows that a FIR filter is also capable of equalizing a directly modulated laser.

In contrast, the influence of the filter memory length, indicated with the number of taps[3], is relatively low for a low Volterra filter order. This means that due to the nonlinear behavior of chromatic dispersion in the electrical domain, only a nonlinear approach can significantly enhance the transmission length of a directly modulated laser system. Here, it was only intended to show the impact of a Volterra post–filter of a directly modulated laser system. The maximum transmission length strongly depends on the operating point of the laser, as was shown in Section 4.2 where the dispersion supported transmission is analyzed.

5.2.4. Pre–Filter

Obtaining the filter coefficients for the pre–filtered system is not as straight forward as for the post–filtered system. The Wiener–Hopf equation (5.20), which estimates the optimum filter coefficients,

[2] first order Volterra filter means linear FIR filter like (5.11)

[3] A tap simply represents a delay line in the filter and thus the filter memory, e.g. four taps are two bits.

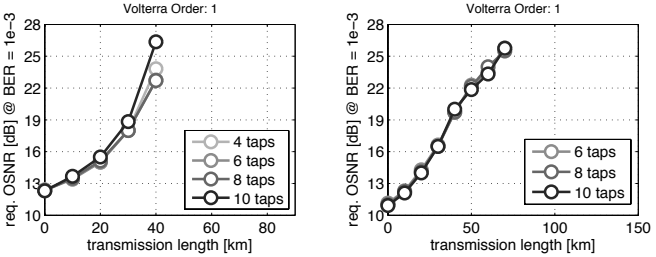

(a) 1st order Volterra, DML target (b) 1st order Volterra, NRZ target

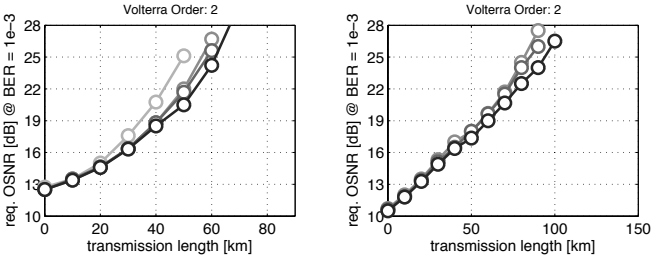

(c) 2nd order Volterra, DML target (d) 2nd order Volterra, NRZ target

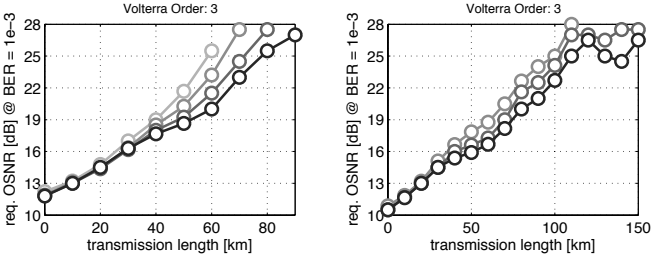

(e) 3rd order Volterra, DML target (f) 3rd order Volterra, NRZ target

Figure 5.9.: Transmission behavior of a directly modulated laser signal with a Volterra post–filter. The Volterra filter is trained for two different signals: A back–to–back directly modulated laser signal (a, c, e) and a biased and modulated NRZ signal (b, d, f) (see Fig. 5.8). The laser chirp is $\alpha = 2$. NOTE: Different scales of the X–axes.

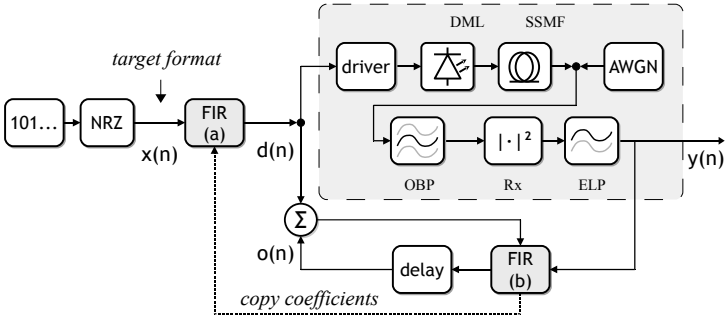

Figure 5.10.: Simulation setup for the indirect learning algorithm to obtain a system pre–filter.

implies that the used FIR filter is "behind" the transmission system. Obviously, this is not the case if a pre–filter is used.

For a commutative system, a simple approach would be to take the optimum post–filter, estimated by the Wiener–Hopf equation, without any changes as a pre–filter. In the optical domain the chromatic dispersion is commutative and a DCF can be used before or after the SSMF. But in the electrical domain and thus with respect to the directly modulated laser, the system is *not* commutative. A post–filter that is optimal for equalizing the received signal does not lead to a correct predistorted signal. This is due to the fact that the fiber transfer function for the optical power depends on the optical input signal (see Section 5.1).

Thus a different approach is taken. The *indirect learning algorithm* presented by Eun et al. [41] was primarily used to linearize amplifiers in transmission systems like satellite links. The principle of the indirect learning algorithm for an optical transmission system is shown in Figure 5.10. First, an electrical target format (illustrated by the NRZ–block) will be generated. This target signal can be ideal or biased and modulated as it is appropriate for

the actual transmission system. The FIR (a) filter will be used as the pre–filter, while the FIR (b) filter is only used to determine the filter coefficients for the FIR (a). The FIR (b) will be trained with the (predistorted) signal $d(n)$ by minimizing $(d(n) - o(n))^2$. The copied coefficients may then lead to a minimized mean square error (MSE) $\overline{(x(n) - y(n))^2}$.

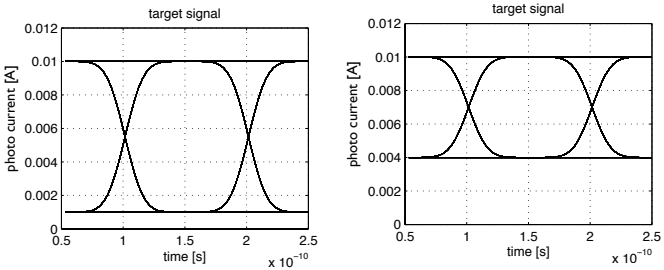

(a) bias 5.5 mA, modulation 4.5 mA (b) bias 7 mA, modulation 3 mA

Figure 5.11.: Electrical NRZ target signal for indirect learning algorithm.

In a typical directly modulated transmission system, the laser injection current $d(n)$ is much different from the optical laser output power. In order to use the system target format $x(n)$ also as the laser injection current (especially in the first iteration, where no FIR (a) filter is used), it is appropriate to relate the target signal to the laser injection current. This is done by the driver block just in front of the directly modulated laser which considers the laser threshold and the slope efficiency of the laser.

In fact, the approach of the indirect learning algorithm fails. Taking a conventionally NRZ signal as the target signal such as

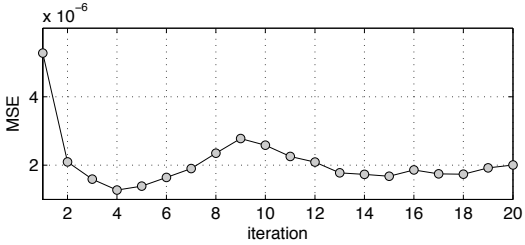

(a) Mean Square Error

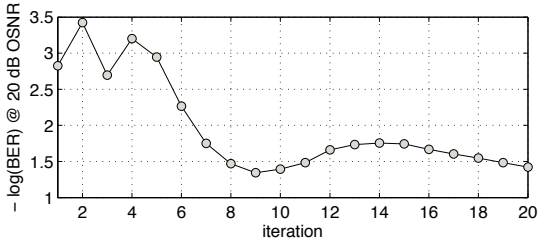

(b) BER

Figure 5.12.: Indirect learning algorithm for pre–filter estimation. Transmission length 200 km, 2nd order Volterra filter, target format: biased with low modulation NRZ (Fig.: 5.11b), OSNR = 20 dB.

ilustrated in Figure 5.11a with a bias current $I_{bias} = 5.5\,\mathrm{mA}$ and a modulation current $I_{mod} = 4.5\,\mathrm{mA}$, the originally positive injection current of the laser becomes partly negative because of the FIR (a) pre–filter. In the simulations, any negative injection current will be set to zero and thus the system may change dramatically. This leads to an unstable, diverging indirect learning algorithm. Additionally, higher order Volterra filters respond relatively sensitive to small input changes. Small changes in their input signals, as if happens if the filter is used as a pre– instead of a post–filter, may lead to an unpredictable behavior of the fil-

ter. Thus, only for a few special configurations of the transmission system and the Volterra filter, the indirect learning algorithm becomes stable.

For a biased target signal with a low modulation ($I_{bias} = 7\,\mathrm{mA}$, $I_{mod} = 3\,\mathrm{mA}$) as in Figure 5.11b and a second order FIR filter with 8 taps (4 bit memory), the algorithm is relatively stable. Figure 5.12a shows the error curve of the indirect learning algorithm for a transmission length of 200 km. The OSNR is 20 dB. The mean square error MSE of the first iteration reflects the non predistorted system, as in the first iteration the FIR (b) will be estimated for the first time and no FIR (a) is used. The MSE decreases up to the 4^{th} iteration by a factor of about 5. After that, the MSE increases again and does not converge to a value lower than the value at the 4^{th} iteration.

In contrast, the BER does not decrease in the same way. Instead, after the 5^{th} iteration, the BER increases, while the MSE stays at a relatively low level, compared to the non predistorted system (first iteration). An explanation for this behavior may be found in Figure 5.13, where the received electrical eye diagrams for different iteration steps are shown. The non pre–filtered system shows a received electrical eye with significant overshoots. Due to the predistortion, the received eye becomes more smooth, the overshoots disappear. But unfortunately, the eye becomes more closed with more iterations and does not open as it would be necessary to reduce the BER.

In summary, the indirect learning algorithm is not capable to estimate a FIR filter to predistort the chromatic dispersion in a directly modulated laser system. The algorithm is stable only for a few special configurations of the transmission system and thus cannot be used to generate a predistorted signal for an arbitrary target signal at the receiver.

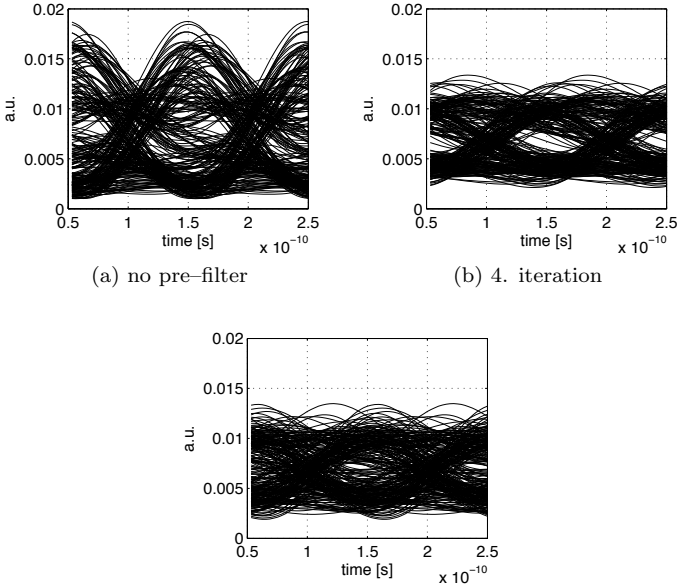

(a) no pre–filter

(b) 4. iteration

(c) 20. iteration

Figure 5.13.: Received electrical eye diagrams for different iteration steps according to Fig. 5.12

5.3. Artificial Neural Network

After the small signal approach in Section 5.1 and the Volterra FIR filter approach in Section 5.2 failed to generate an applicable electronic predistortion for a directly modulated laser system, a novel technique for signal predistortion in optical transmission systems will be introduced. The novel technique is based on an artificial neural network as a nonlinear filter and the particle swarm algorithm as the optimization algorithm.

An artificial neural network (ANN) is a nonlinear system inspired by the biological nervous system. It consists of processing elements, so called neurons, which are interconnected to solve special problems like pattern recognition or signal processing [32]. In contrast to the well defined Volterra filter, there are many different neural networks, designed for many different applications and thus, many different algorithms exist to train the neural network. In the following two sections, the feed-forward neural network and the particle swarm algorithm as the optimization algorithm will be introduced.

5.3.1. Feed–forward Neural Network

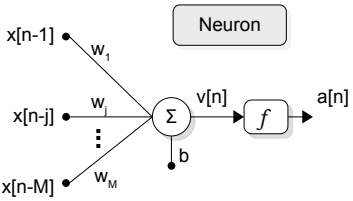

Figure 5.14.: A neuron consisting of weights w, a bias b and a typically nonlinear transfer function f

The feed–forward neural network is the simplest type of an artificial neural network [32]. Like all artificial neural networks, it is based on neurons. A typical neuron is shown in Figure 5.14. Similar to a FIR filter, different inputs are added with a weight factor w. The sum is then biased and typically fed into a nonlinear transfer function f. The transfer function should be restricted, i.e the output value of the neuron, or the complete neural network, is never outside a specified range. This aspect of a neural network is particularly interesting for the particle swarm algorithm later introduced to train the neural network. A typical transfer function is the so called sigmoid function:

$$f(x) = \frac{1}{1 + \exp(-x \cdot c)} \tag{5.25}$$

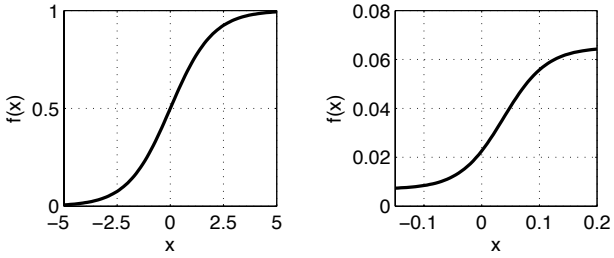

Figure 5.15.: Sigmoid functions: (a) In general by eq. (5.25) with $c = 1$ and (b) the used customized function (5.26).

To adapt the function to the intended application, the sigmoid

function is rewritten as follows:

$$f(x) = \left(\frac{1}{1 + \exp(-(cx - k))} \cdot (d_{max} - d_{min}) \right) + d_{min} \quad (5.26)$$

with d_{max} being the upper and d_{min} being the lower bound of the function, k being a parameter that represents the slope of the function and the parameter c with the relation:

$$c = (-\ln(\frac{d_{max} - d_{cent}}{d_{cent} - d_{min}}) + k)/d_{cent}. \quad (5.27)$$

with d_{cent} the center point of the function (where $f(d_{cent}) = d_{cent}$).

Figure 5.15 shows the general and the customized sigmoid function. The parameters for the customized sigmoid function used in the later simulations are: $d_{max} = 65 \cdot 10^{-3}$, $d_{min} = 7 \cdot 10^{-3}$, $d_{cent} = 35 \cdot 10^{-3}$ and $k = 1$. As shown in Figure 5.15 the customized sigmoid function restricts the output of the neural net, and thus the predistorted injection current, to values between 7 mW and 65 mW.

Mathematically, the output of neuron $a[n]$ may be described as follows:

$$a[n] = f\{v[n]\} \quad (5.28)$$

$$= f\left\{ \sum_{j=1}^{M} (w_j \cdot x[n-j]) + b \right\} \quad (5.29)$$

Fundamentally, an artificial neural network may consist of only one neuron, but this would restrict the ability to approximate any nonlinear system. The multi–layer feed–forward neural network, shown in Figure 5.16 [32], consists of a number of neurons in three layers, which are interconnected in a feed–forward manner. Thus,

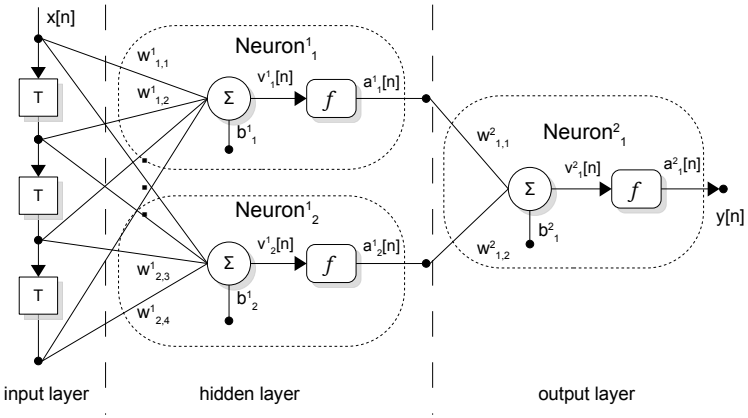

Figure 5.16.: Feed–forward neural network.

the information moves only in one direction, without any kind of feedback. The three layers are the input layer, the hidden layer and the output layer. In the input layer, each delayed sample value of the input signal is fed to a very simple neuron without weights, bias or transfer function. From that input layer, the *input* neurons are interconnected to the hidden layer. The example in Figure 5.16 has two neurons in the hidden layer, but the hidden layer can consist of as many neurons as needed. The last layer is the output layer, where all neurons from the hidden layer are connected to one ore more neurons, as it is required for the special application. In Figure 5.16, $w^k_{n,j}$ refers to the k^{th} layer, the m^{th} neuron in the depicted layer and the j^{th} input for the neuron. The neural network shown in Figure 5.16 may be described as follows:

$$y[n] = f\left\{v_1^2[n]\right\} \tag{5.30}$$

$$= f\left\{\sum_{i=1}^{N}(w_{1,i}^2 \cdot a_j^1[n]) + b_1^2\right\} \tag{5.31}$$

$$= f\left\{\sum_{i=1}^{N}\left(w_{1,i}^2 \cdot f\left\{\sum_{j=1}^{M}\left(w_{i,j}^1 \cdot x[n-j]\right) + b_i^1\right\}\right) + b_1^2\right\} \tag{5.32}$$

where $a[n]$ is defined in (5.29) for an arbitrary neuron in the neural network, N is the number of neurons in the hidden layer and M is the number of weights w of neurons in the hidden layer (i.e. memory of the neural network).

The universal approximation theorem by Hornik [42] states that any continuous function can be approximated arbitrarily close with that kind of neural network and a finite number of neurons in the hidden layer. This is valid only for a restricted class of transfer functions, like the used sigmoid function. This means that the artificial neural network is able to generate *any* signal predistortion, and the challenge is to *find* the most appropriate neural network (and thus the coefficients) to predistort the chromatic dispersion for a given optical transmission system.

In order to keep the effort of finding the right neural network parameters low, the aim should be to use as few neurons in the hidden layer as possible. The neural networks used in this work have about three to five neurons in the hidden layer with about 6 to 10 weights w. Thus the total number of coefficients of the used neural networks are about 20 to 60 [4].

[4] for example: (3 neurons × (8 weights + 1 bias)) + (3 weights + 1 bias) = 31 coefficients

5.3.2. Particle Swarm Algorithm

One of the most important training algorithms for neural networks is the so called backpropagation[5] algorithm [32]. This algorithm requires an *imaginary* teacher that *knows* the desired neural network output for an arbitrary input. In case of a directly modulated laser system, the predistorted signal that pre–compensates the chromatic dispersion is unknown. In a more general approach for the training, the coefficients of the neural network are not trained for a given target signal and thus for a special predistorted signal. Instead, the optimization of the neural network should lead to a good system performance, e.g. a low BER for a given OSNR. Or more mathematically formulated: Minimize the system fitness function (BER) with respect to the coefficients of the neural net. For that purpose, a number of different algorithms exists.

The very famous gradient descent algorithm (steepest descent) uses the negative gradient of the fitness function to "walk" in steps from a starting point towards a local minimum. In case of fitness functions with only one minimum, that algorithm may be a good approach, as it can determine the local minimum relatively accurate, depending on the step size of the algorithm. For nonlinear fitness functions with many different local minima, as the predistorted system, the gradient descent algorithm fails. The algorithm only finds a minimum close to the starting point. Furthermore, it cannot be decided if the found minimum is local or global.

Finding the global minimum (or maximum) for a given problem is much more challenging. Some of the most important global optimization algorithms are inspired by natural mechanisms like evolution or swarm intelligence [43, 44], such as the particle swarm optimization algorithm [45, 46]. The particle swarm algorithm is based on the behavior of a bird flock. Most people know the following situation. Someone is sitting on a bench in a park and is starting to feed a pigeon with bread–crumbs. After a while a second pigeon is coming, and it does not take much time until a

[5] abbreviation for: backwards propagation of errors

small pigeon flock is landing next to the bench and feed the bread–crumbs from the ground. From a mathematical point of view, the bird flock found the global maximum of the *feed-function*, which is exactly what a global optimization should do. To find that optimum, each pigeon of the flock orients itself towards its own knowledge of the explored area (where most food is to be found) and the knowledge of his neighbors. The particle swarm algorithm is working the same way. Multiple particles, i.e. sets of neural network coefficients, are *flying* around in a multidimensional space with the objective to find the coefficients of the neural net that lead to a minimum BER. In doing so, each particle has the knowledge of two things:

- The place (i.e. the neural network coefficients) where it gained the best system performance so far (local optimum).
- And the place where the whole swarm or just a few neighboring particles gained the best system performance so far (global optimum).

This information will be used to accelerate the particle $\vec{P}[n]$, which represents the coefficients of one neural net, at each iteration of the algorithm and thus to adjust the direction where the particle is *looking* for a system optimum:

$$\vec{v}[n+1] = g\,\vec{v}[n] + c_1\xi_1(\vec{P}_{best} - \vec{P}[n]) + c_2\xi_2(\vec{G}_{best} - \vec{P}[n]) \tag{5.33}$$

Here, $\vec{v}[n+1]$ is the new updated particle velocity, $0 \leq g \leq 1$ is an inertia parameter, c_1, c_2 are cognitive and social parameters similar to a step size, $0 \leq \xi_1, \xi_2 \leq 1$ are random values and $\vec{P}_{best}$ and $\vec{G}_{best}$ are the so far local and global optima, respectively. The new particle is then:

$$\vec{P}[n+1] = \vec{P}[n] + \vec{v}[n+1] \tag{5.34}$$

The principle of the partical swarm optimization algorithm as it is formulated in (5.33), (5.34) is graphically shown in Figure 5.17.

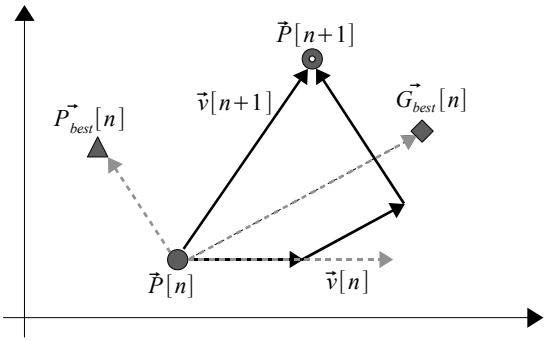

Figure 5.17.: Graphical illustration of the particle swarm algorithm.

Without the inertia parameter g in (5.33), the particle swarm would not converge to an area of interest, where the global optimum is assumed. Instead it would spread out and the algorithm may not converge. But this also means, with a too small inertia parameter, the swarm searches only in a relatively small area compared to the predetermined optimization area, and thus may only find a relatively poor system optimum. The so far global optimum $\vec{G}_{best}$ may be based on the optimum of a number of neighbor particles or, as done in this work, may be based on the whole swarm. The latter approach leads to a faster convergence of the algorithm, which may be of note if the simulation of the system takes much time. To prevent a too fast movement of the whole swarm to the current global optimum of the optimization process, in this work not only the so far swarm optimum is considered to calculate the movement of the single particles, but also the current second, third etc. best particle of the swarm. This approach converges much faster than the *neighbor* approach, but leads to similar optimization results.

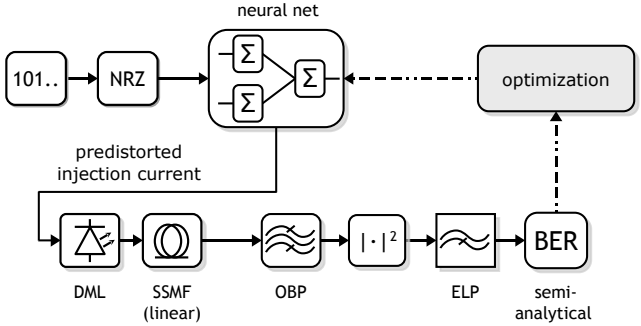

Figure 5.18.: Optimization scheme for an artificial neural net and the optical transmission system.

5.3.3. Optimization Setup

In Figure 5.18 the optimization setup for the neural network optimization is shown. An NRZ modulated signal is fed into the neural network. The predistorted output of the neural net is used to modulate the laser.

In order to apply the particle swarm algorithm to the neural net, the coefficients of the neural net are a particle of the swarm algorithm. As the particle swarm algorithm is based on a swarm, or a group of different particles, in one iteration step of the algorithm multiple different neural network coefficients (multiple particle) are used to estimate the BER of the system. For the next iteration the coefficients will be changed by the particle swarm algorithm, corresponding to the estimated BER. The optimization terminates after a previously defined number of iterations. The parameters for the optical transmission systems that will be predistorted are given in section 4.1 with two differences: the BER estimation and the used bit sequence.

To reduce the computational effort, the BER estimation is done

distance [km]	taps M	neurons in the hidden layer N	particles	iterations
50	6	3	70	120
100	6	3	70	120
150	6	3	70	120
200	8	3	100	150
250	8	4	150	200
300	10	4	150	200
350	8	5	150	300

Table 5.1.: Used neural network structure and particle swarm optimization parameters to obtain the best system performance for different predistortion distances. Laser chirp $\alpha = 2$.

semi–analytically. With respect to the inter symbol interference (ISI), the bit error probability is estimated with a noise distribution at the receiver assumed to be normal Gaussian shaped [47]. In fact, the noise distribution is gaussian only in the optical domain and becomes a non central χ^2 distribution in the electrical domain [48]. But for a fast estimation of the optimization criterion of the system performance, the Gaussian assumption may be accurate enough. When the optimization is terminated, the BER will be estimated again with the found neural network coefficients and the Monte Carlo method, as it is done for other simulations in this work. The used bit sequence for optimization is a 2^7 or 2^8 de Brujin sequence with 128 (256) bit. For a transmission length of up to 350 km, this bit sequence may be too short to consider all signal degradations induced by the chromatic dispersion, but it is adequate to estimate the optimization criterion. For the second BER estimation after the optimization, a de Brujin sequence 2^{11} (2048 bit) is used.

distance [km]	taps M	neurons in the hidden layer N	particles	iterations
50	8	3	100	150
100	8	3	100	150
150	8	3	100	150
200	8	3	100	150
250	8	3	150	200
300	10	3	150	200
350	10	4	150	200

Table 5.2.: Used neural network structure and particle swarm optimization parameters to obtain the best system performance for different predistortion distances. Laser chirp $\alpha = 3$.

The used neural network consists of three to five neurons in the hidden layer and 6 to 10 taps (delay lines), depending on the transmission length of the system, as shown in Table 5.1 and in Table 5.2 for a laser chirp $\alpha = 2$ and $\alpha = 3$, respectively. The input signal (discrete–time) of the neural net is sampled with 2 samples per bit. The transfer function (eq. (5.27)) is the same for all neurons. As mentioned earlier, one advantage of a sigmoid transfer function for the neural network is that it is restricted. This means that no matter what the actual coefficients of the neural network are during the optimization, the output is always in a prior defined range. This makes the particle swarm optimization more stable than it would be possible with a Volterra filter.

To start the particle swarm optimization algorithm, an initial set of neural network coefficients has to be randomly chosen. Even with a restricted neuron transfer function and a boundary area of the coefficients, it may happen that the resulting predistorted laser

injection current is almost a DC signal. This DC laser injection current without modulation leads to a $BER \approx 0.5$ and a plateau like area in the fitness function (BER) of the optimization system. A small change of some coefficients of that signal does not lead to a better system performance. But the optimization of a plateau–like function is very difficult, as it is very hard to distinguish different system values and thus different input values of the system. Therefore, only those initial coefficients for a neural net are taken, which does not lead to an unmodulated injection current.

As already described, the performance criterion of the particle swarm optimization is the BER. This means, the optimization does not predistort a given target format (e.g. a biased NRZ format) but finds the the most *predistortable* target signal and thus the predistorted laser injection current. This is a big advantage of that approach, because the transmission performance of a directly modulated laser depends strongly on the laser bias and modulation conditions.

The settings for the particle swarm algorithm depend on the transmission length. The longer the transmission distance, the more particles and the more iterations are necessary for the algorithm to converge. Typically, the number of particles is 70 to 200 and the number of iterations is between 120 and 400 as shown in Table 5.1 and in Table 5.2 for a laser chirp $\alpha = 2$ and $\alpha = 3$, respectively. The inertia parameter is $g = 0.5$ and the cognitive and social parameters are $c_1 = c_2 = 1.4$.

In order to prove if the optimum found by the particle swarm algorithm is at least a local optimum, the pattern search algorithm[6] [49] is used. Interestingly, almost every optimum found by the particle swarm algorithm is a local optimum. If that is not the case, the optimization result is very close to a local minimum.

[6]The pattern search algorithm is based on the gradient descent algorithm, but does not calculate any derivative of the fitness function. A more detailed description is given in [49].

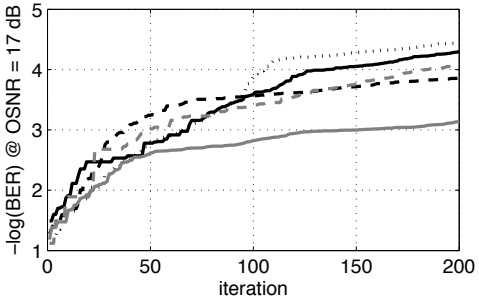

Figure 5.19.: Error function for five different optimizations of the same predistorted system (300 km, $\alpha = 2$, taps $M = 10$ and neurons $N = 4$ (49 coefficients), 150 particles,).

Because the particle swarm algorithm is a non–deterministic optimization approach (and because the fitness function has many different optima), each optimization may lead to a different result. In Figure 5.19 five different error functions (BER) of the particle swarm optimization for the same predistortion system are shwon. As can be seen, the particle swarm algorithm converges, but leads to five different results in five optimization runs . Thus, every system is simulated about 3 to 8 times, in order to find the best optimization results. Figure 5.20 shows optimization performance for two predistorted signals for 150 km and 300 km transmission distance. As the predistorted signal for 150 km converges relatively fast, the predistorted signal for 300 km takes much more iterations. The reason are the different numbers of neural network coefficients (25 coefficients for 150 km transmission and 49 coefficients for 300 km transmission).

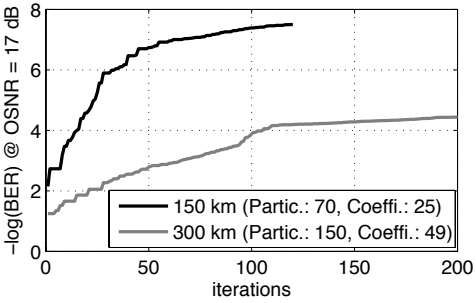

Figure 5.20.: Error function (BER) of the particle swarm algorithm for two predistorted signal (150 km and 300 km). Laser chirp $\alpha = 2$.

5.3.4. Optimization Results

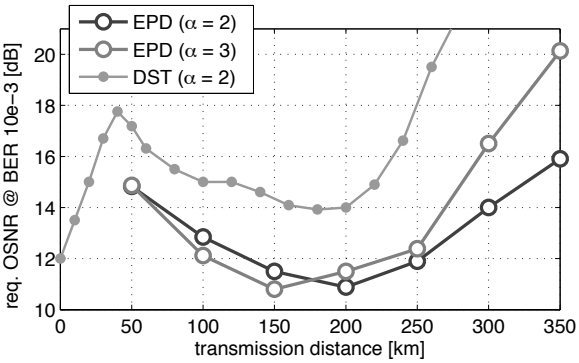

Figure 5.21.: Electronically predistorted transmission system (EPD) in comparison to a dispersion supported transmission system (DST).

Based on the optimization setup in Section 5.3.3 Figure 5.21 shows the optimization results for the predistorted directly modulated laser transmission system with two different laser chirp factors. The optimization is done for a transmission distance between 50 km and 350 km. A longer system transmission ($\geq$ 400 km) leads to a required OSNR $>$ 30 dB (at BER $= 10^{-3}$).

The system performance for the predistorted system shows a considerable improvement not only compared to the NRZ system (see section 4.1), but also compared to a dispersion supported transmission system. The best system performance for a laser chirp $\alpha = 2$ is achieved at 200 km with a required OSNR $= 11$ dB (BER $= 10^{-3}$) (for $\alpha = 3$ at 150 km also with OSNR $= 11$ dB). Thus, the predistortion leads to a negative OSNR penalty compared to the NRZ back–to–back signal of 0.5 dB (and 2 dB for $\alpha = 3$) (compare with Figure 4.3a).

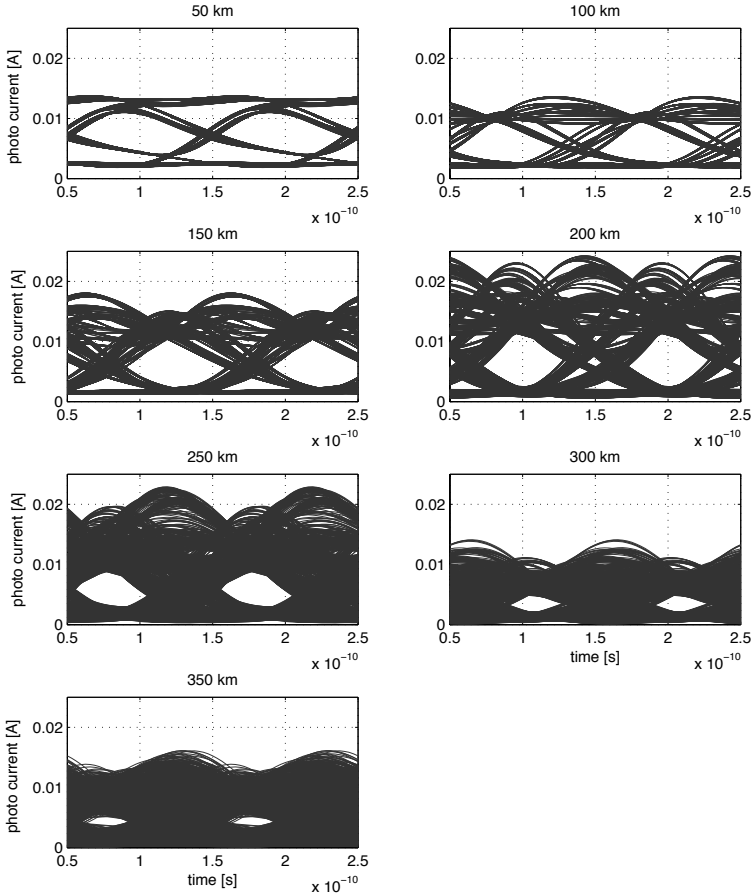

Figure 5.22.: Eye diagrams of the electrical signal for the predistorted signals for different transmission distances (laser chirp $\alpha = 2$).

The maximum transmission of the predistorted system is about 350 km, which is an improvement of the transmission distance compared to the dispersion supported transmission of about 100 km. Additionally, the required OSNR of the predistorted system is always about 2 dB better than that of the dispersion supported transmission system.

In a range between 50 km and 250 km, both predistorted systems ($\alpha = 2, 3$) differ only slightly, with a better performance at short transmission distances for the higher chirped system. The performance of the predistorted system with a laser chirp $\alpha = 2$ at a distance ≥ 200 km is better than the predistorted system with $\alpha = 3$, with a considerable improvement for a distance ≥ 300 km.

Figure 5.22 shows the received electrical eye diagrams from 50 km to 350 km transmission distance (chirp $\alpha = 2$). The received eye diagrams are very different in terms of overshoot, jitter and eye opening. That is not surprising, because the only optimization criterion is the BER and not any signal shape.

Beside the eye diagrams of the received signals, it is interesting to see the time signal of the predistorted signal and the received signal after transmission. Figure 5.23a shows the predistorted laser modulation current for a transmission distance of 200 km and a laser chirp of $\alpha = 2$. Figure 5.23b shows the optical power signal of the laser output and the optical power signal after fiber transmission. A relatively low modulation of the laser output increases after fiber transmission due to FM–AM[7] conversion by chromatic dispersion (see Section 4.2). The electrical receiver signal, which is optically and electrically filtered, is much smoother than the transmitted optical signal. In fact, without the receiver filters, the predistorted signal would not lead to a good system performance, as the filters are included in the optimization setup.

Table 5.1 and Table 5.2 show the used neural network configuration to achieve the best system performance. As the particle

[7] frequency modulation – amplitude modulation

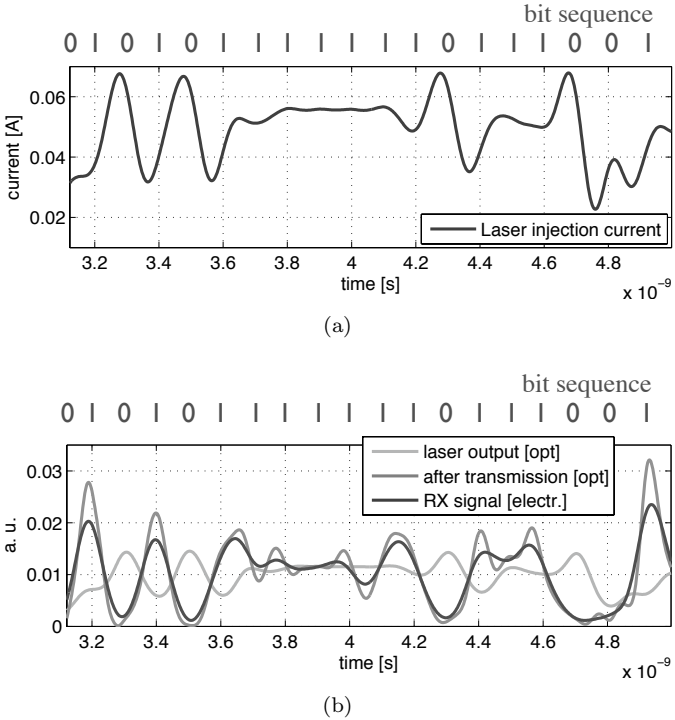

Figure 5.23.: Sample signals for a predistortion of 200 km. a) predistorted laser injection current b) laser output signal, optical signal after transmission and filtered electrical signal at the receiver. Laser chirp $\alpha = 2$.

swarm optimization algorithm is not deterministic and the optimization is time–consuming, there might be other more suitable neural network configurations for certain transmission distances, but the overall trend of the system should not change. Up to a transmission distance of 350 km, a memory length of the neural network of 4 to 5 bit is sufficient to achieve a superior system behavior, and the higher the transmission distance, the more neurons in the hidden layer are necessary.

Dispersion Tolerance

In addition to the maximum transmission length, the dispersion tolerance of the predistorted signals is analyzed. Figure 5.24 shows the dispersion tolerance around the optimized transmission length for different predistorted signals without changing the optimized coefficients of the neural network (laser chirp $\alpha = 2$). The typical dispersion tolerance with a penalty of 2 dB is about 100 km, for long transmission distances a little bit lower. This is a remarkable result, as the dispersion tolerance for the NRZ system (section 4.1) is only about 10 km.

The reason for the good dispersion tolerance and the high system performance may also be found in the optical power spectrum. Figure 5.25 shows the optical power spectrum for three different predistorted signals. The inset in that figure shows the spectral width ($2 \cdot \sigma$). As described in section 4.1, for the NRZ directly modulated laser system, the optical power spectrum spreads out due to the chirp, and the spectral components of the "1" and "0" symbols of the signal can be seen in the spectrum as two peaks at about ± 5 GHz. In case of the predistorted signals, the distance between the peaks of the "1" and "0" symbols becomes smaller. This may be due to a reduced modulation index of the predistorted signal. As can be seen in the inset, the higher the transmission distance, the narrower the optical power spectrum. Compared to the NRZ laser system (Fig.: 4.3b), the spectral width is halved at

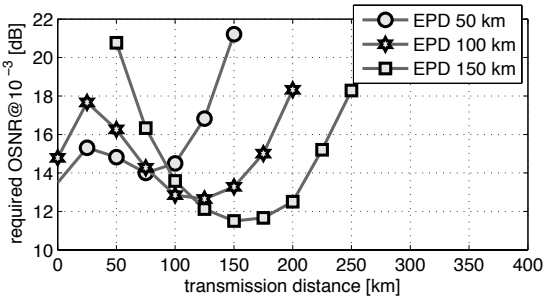

(a) 50 km to 150 km

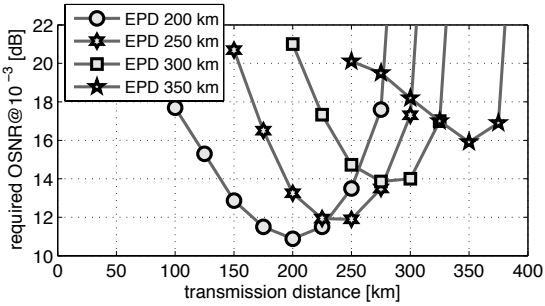

(b) 200 km to 350 km

Figure 5.24.: Dispersion tolerance for different predistorted signal. Every line illustrates the dispersion tolerance of one denoted predistorted signal (D = 16 ps/km/nm, α = 2)

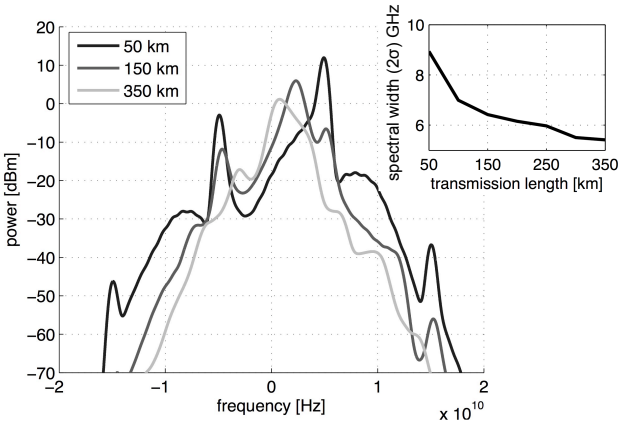

Figure 5.25.: Optical power spectrum of the predistorted signals. The inset shows the spectral width for the predistorted signals. (Laser chirp $\alpha = 2$.)

high transmission distances.

Impact of Fiber Nonlinearities

To analyze the signal predistortion together with single channel fiber nonlinearities, the nonlinear Schrödinger equation has to be used (3.26). For this purpose the *SSPROP - Split Step Fourier Propagation Software* by the University of Maryland (USA) is used. The program is based on the Split Step Fourier algorithm [10] and can be invoked directly from Matlab, the simulation software used for this work.

The simulation setup remains almost the same as for the previous simulations. The only differences are the nonlinear fiber and the noise free fiber amplifier after every 100 km. The fiber loss is 0.2 dB/km and the nonlinear coefficient of the fiber is $\gamma =$

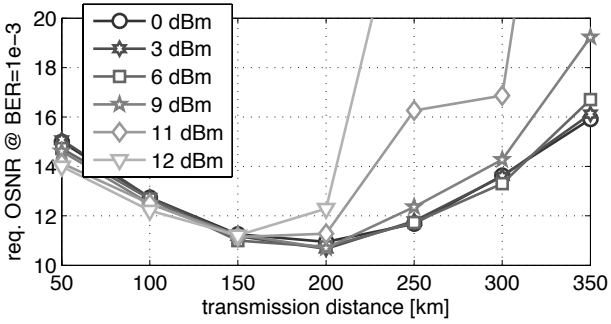

Figure 5.26.: Influence of single channel fiber nonlinearities for different optical fiber launch powers. (Laser chirp $\alpha = 2$)

$1.3144\,\mathrm{W^{-1}km^{-1}}$. Figure 5.26 shows the simulation results for different optical fiber launch powers between 0 dBm and 12 dBm. A launch power of up to 6 dBm does not change the required OSNR significantly compared to the linear system. However, a higher launch power leads to a noticeably higher required OSNR. With 12 dBm launch power the maximum transmission distance is about 200 km and thus 150 km less than for the linear system.

While the predistorted system suffers from fiber nonlinearities, the dispersion supported transmission system takes advantage of the nonlinearities (SPM) [50]. This is due to the fact that the predistorted system is optimized only for a linear system. Taking instead a nonlinear system as the training system, which would take significant more simulation time as available, the performance of the predistorted system may increase.

5.3.5. Experimental Results

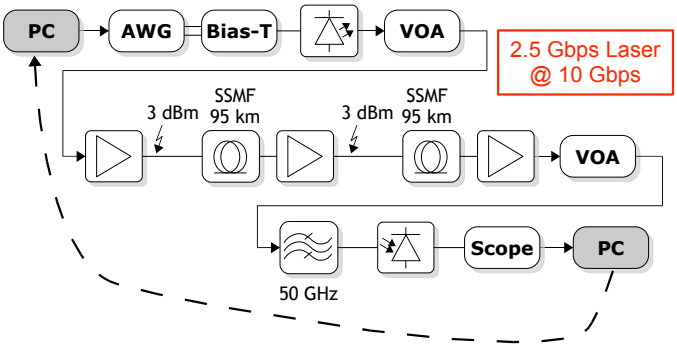

Figure 5.27.: Experimental setup. The neural network and the particle swarm algorithm is implemented in the PC.

For experimental verification of the signal predistortion, no directly modulated laser for 10 Gbit/s has been available and thus a directly modulated laser for 2.5 Gbit/s had to be taken (Agere D2555). A transmission system with that laser suffers from bandwidth limitation and may not be representative for common 10 Gbit/s transmission systems. Therefore, the aim of the experiments is to prove the concept of signal predistortion of directly modulated lasers.

The experimental setup is shown in Figure 5.27. As in the simulations, the personal computer (PC) controls the optimization algorithm (particle swarm optimization) to find the correct neural network coefficients. The artificial neural network is also implemented in the PC, such that the predistorted laser injection current (output of the neural network) can be sent directly from the PC to an arbitrary waveform generator (AWG). The AWG works with 20 GSamples/s and a resolution of 8 bit and outputs

transmitted length	predistorted length	OSNR [dB]	BER	errors
95 km	95 km	33,6	$8,3 \cdot 10^{-4}$	272
95 km	190 km	33,6	$5,6 \cdot 10^{-4}$	182
190 km	95 km	33,0	$2,6 \cdot 10^{-2}$	4940
190 km	190 km	33,0	$9,9 \cdot 10^{-4}$	325
290 km	190 km	30,6	$5,0 \cdot 10^{-2}$	9912

Table 5.3.: Measured BER for different predistorted signals.

the laser modulation current divided into a DC and an AC part. The transmission line is based on one or two fiber spans, consisting each of a 95 km fiber with about 18 dB attenuation and 1620 ps/nm dispersion and an EDFA[8]. The fiber input power is 3 dBm. At the end of the transmission link, the signal is optically filtered by a 50 GHz band pass and detected by a p–i–n photodiode. A 20 GSamples/s digital oscilloscope is used to sample the received signal and to feed it to the PC for system optimization. The oscilloscope averages the received electrical signal while the particle swarm optimization is working in order to eliminate the influence of the noise. For performance reasons of the optimization, the bit error probability, beeing the fitness function of the particle swarm algorithm, is calculated at the PC with a noise distribution at the receiver assumed to be normal Gaussian shaped (compare Section 5.3.3).

After the neural network optimization is finished, the BER for a given OSNR of the predistorted system is measured with the digital oscilloscope. Thus, only a restricted number of errors can be counted to estimate the BER. The OSNR is measured with an optical spectrum analyzer.

Table 5.3 shows the measured BER for a given OSNR. The maximum achieved transmission length with a predistorted signal is 190 km with BER $= 9.9 \cdot 10^{-4}$ at OSNR $= 33.0$ dB. That is more than 20 dB worse than the simulation results. Unfortunately, a transmission over 290 km could not be shown experimentally. The considerable differences between experiment and simulation, may be causes by the poor modulation bandwidth of the used laser. But achieving a transmission distance of 190 km with a laser that was specified for 2.5 Gbit/s is still remarkable. The predistorted signal also shows a high dispersion tolerance towards shorter transmission distances. Comparing the two signals transmitted over 95 km, the predistorted signal for 190 km shows a better system performance than the signal predistorted for 95 km. This is due to the non deterministic behavior of the particle swarm optimization algorithm, which means the found predistorted signal for 95 km is *not* the optimum.

However, compared to results by Papagiannakis et al. [51], where a 2.5 GBit/s laser was also modulated at 10 Gbit/s, but post–equalized with a FFE/DFE structure, a transmission distance of 190 km is an improvement of about 50 km.

Figure 5.28 shows the received eye diagrams for a non predistorted back–to–back signal and a predistorted signal for 190 km (and also 190 km transmitted). As can be seen, the back–to–back eye diagram 5.28a is relatively poor due to the limited laser bandwidth. The predistorted signal found by the optimization algorithm (Figure 5.28b) is highly biased, which may be due to the increased bandwidth at highly biased lasers.

[8] erbium doped fiber amplifier

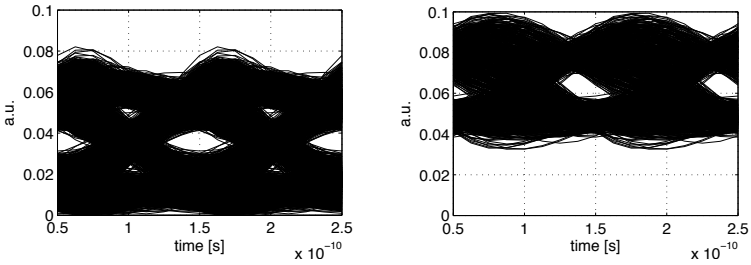

(a) back–to–back, no predistortion (b) after 190 km, (190 km predistorted)

Figure 5.28.: Measured received eye diagram for a 2.5 Gbit/s laser at 10 Gbit/s. The signal is averaged for noise reduction.

CHAPTER 6

SIGNAL PREDISTORTION COMBINED WITH POST–PROCESSING

Electronic dispersion compensation at the receiver is a widespread technique to overcome transmission restrictions due to chromatic or modal dispersion. It is standardized by the IEEE for short range multimode applications [52] and is also used in single mode applications [53, 54].

There are mainly two approaches for the electronic dispersion compensation using a direct detection receiver which are briefly introduced in this chapter, before they are studied in conjunction with signal predistortion.

6.1. FFE/DFE

The feed–forward / decision feed–back equalizer (FFE/DFE) [54, 55, 34] consists of a transversal filter structure, as described in section 5.2. The feed–forward section (FFE) is able to compen-

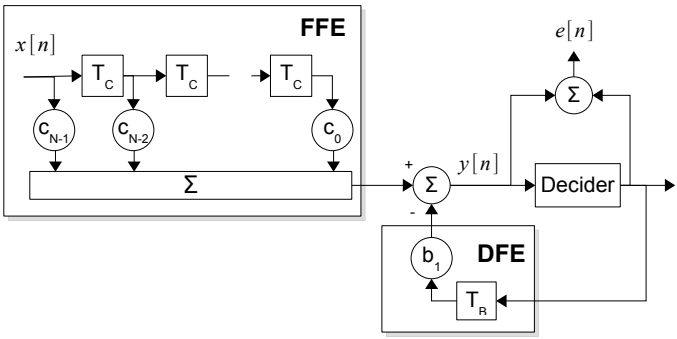

Figure 6.1.: Feed–forward - decision feed–back equalizer structure (FFE/DFE).

sate linear distortions of the signal (figure 6.1). In this work, the signal is delayed by the delay stage $T_C = 1/(2B)$, with a signal bit $B = 10\,\mathrm{Gbit/s}$. The feed–back section (DFE) is also based on a transversal filter, but with only one filter weight and a delay T_B of one bit. The input of the feed-back section is made up of previously detected symbols. The idea of the feed–back section is to subtract the inter–symbol interference produced by previously detected symbols from the estimate of future symbols [34]. A very important aspect of the FFE/DFE structure is the blind estimation capability. According to the mean square error (MSE), based on the error $e[n]$ between an equalized and a detected symbol, the structure coefficients are set up. Thus, no additional training sequence is necessary to train the DFE/FFE structure for a given transmission system. The optimization algorithm used in this work is the recursive least square algorithm (RLS) that is based on a cumulative error [34]:

$$J[n] = \sum_{i=1}^{n} \lambda^{n-i} (e[i])^2 \tag{6.1}$$

Here, $J[n]$ is the fitness function, which is optimized by the RLS algorithm, λ is a forgetting factor close to but less than one and $e[n]$ is the error as depicted in Figure 6.1. The forgetting factor is $\lambda = 0.999$ for the numerical analysis of the DFE/FFE structure in Section 6.3

6.2. MLSE

In addition to the DFE, the maximum likelihood sequence estimation MLSE (or sometimes maximum likelihood sequence detection MLSD called) is a very popular approach of an electrical equalizer to reduce the effect of chromatic dispersion [56, 57]. Agazzi et al. [58] showed that the MLSE outperforms the DFE especially due to the ability to compensate nonlinear distortions.

The first task (demodulation) of the MLSE is to choose from a received noisy sequence $Z = \{z_k, z_{k+1}, \cdots\}$ the *most likely* candidate sequence $U = \{u_k, u_{k+1}, \cdots\}$, which is an ISI distorted sequence but noiseless [59]:

$$p(Z|U^{(j')}) = \max_{j} \; p(Z|U^{(j)}) \tag{6.2}$$

with $j = 1, 2, \cdots, 2^K$ the number of considered system states, where K is the number of considered bits for a sequence. p is the conditioned probability density function (conditioned pdf). Due to the exponentially growing number of possible sequences $\{U^{(j)}\}$, a *brute force* comparison attempt to find the most likely sequence may take too much computational effort. Here, the Viterbi algorithm [60, 61] is much more efficient, as it can quickly discard sequences or trellis paths[1] that are extremely unlikely to be the wanted sequence/path $U = \{u_k, u_{k+1}, \cdots\}$. The decision of the

[1] The concept of trellis will not be explained, as it can be found in various publications like [59].

maximum likely path is based on the summed branch metric of a path, where the metric is based on logarithmic probabilities.

Another task of the MLSE is the decoding of the demodulated signal. Due to chromatic dispersion, the transmitted signal is smeared, which means the information from one bit is also transfered to adjacent bits. Thus the transmitted optical signal is encoded by the chromatic dispersion of the optical fiber. Going backwards through the states of the maximum likely path, an estimate of the transmitted bit sequence can be constructed.

The path metric of the used MLSE and thus the probability density function is based on a prior estimated histogram of the states. The histogram has a resolution of 6 bit. The tails of the probability density function which can not be represented by the histogram are approximated by a second order polynomial. The input signal of the MLSE is sampled with 2 sample per bit.

6.3. Predistortion & Post–equalization

Figure 6.2 shows the system performance of a FFE / DFE with 6 taps at the FFE and one tap at the DFE part and an MLSE with 4 and 16 states (no additional predistortion). The system performance is compared with a standard system without post–equalization. As already published [51, 62], the FFE/DFE structure may double the transmission distance of a directly modulated laser which leads to a transmission distance of about 50 km. The improved back–to–back performance of the FFE/DFE results from the narrow optical receiver filter. Due to the chirp $\alpha = 2$ the back–to–back signal is slightly distorted by the optical filter and can be improved by the FFE/DFE equalizer (see Section 4.1).

Compared to the results of the FFE/DFE equalizer, the maximum transmission distance of both MLSEs is larger. Even the 4 state MLSE (2 bit memory) outperforms the FFE/DFE structure. The maximum transmission distance of the 16 state MLSE (4 bit memory) is about 140 km (req. OSNR $\approx$ 20 dB). Fludger

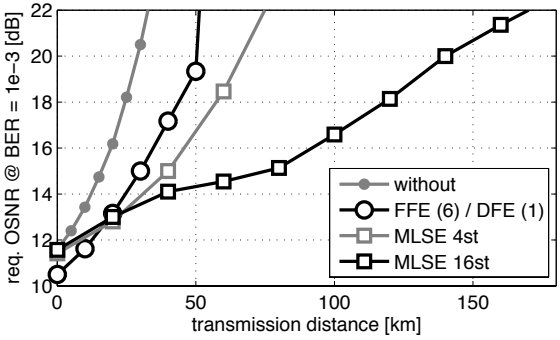

Figure 6.2.: System performance of a directly modulated laser system without equalizing (bulk) and with a FFE / DFE and MLSE equalizer (no additionally signal predistortion $\alpha = 2$).

et al. [63] reported a simulated maximum transmission distance of about 400 km with a 32 state MLSE. The difference is mainly caused by (despite the more states) from the high bias current and the smaller extinction ratio in [63].

In Figure 6.3 the simulation setup of a predistorted system with post–equalization is shown. The previously optimized neural net (optimized without post–equalization) is used to generate the predistorted signal while the EDC block (FFE/DFE or MLSE) equalizes the received signal. In order to analyze the performance of the post–equalization, the predistorted signal for a specific transmission distance is transmitted over a length shorter and longer than the target length.

The simulation results are shown in Figure 6.4 and are discussed with respect to different aspects:

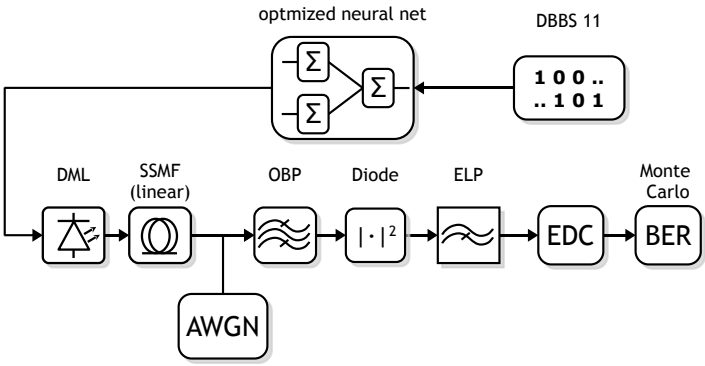

Figure 6.3.: Simulation system with prior optimized neural net and an EDC unit (FFE/DFE or MLSE).

- The EDC only slightly improves ($\approx$ 1 dB) the req. OSNR for the initially predistorted transmission distances for target distances of 50 km to 300 km. Only for a transmission distance of 350 km with a predistortion for the same distance, the 16 state MLSE improves the performance by more than 3 dB. This indicates that the predistortion for 350 km may not be optimal, because an optimal predistorted signal should be ISI free and therefore, an MLSE should not be able to improve the performance further.

- The improvement by the FFE/DFE is only marginal for most of the predistorted signals compared to the inherent dispersion tolerance of the signal predistortion (but shows similar performance as with a non predistorted system).

- The 4 state MLSE improves the maximum transmission distance by up to 100 km especially at lower initially predistorted distances, which is much more than in a non predistorted system.

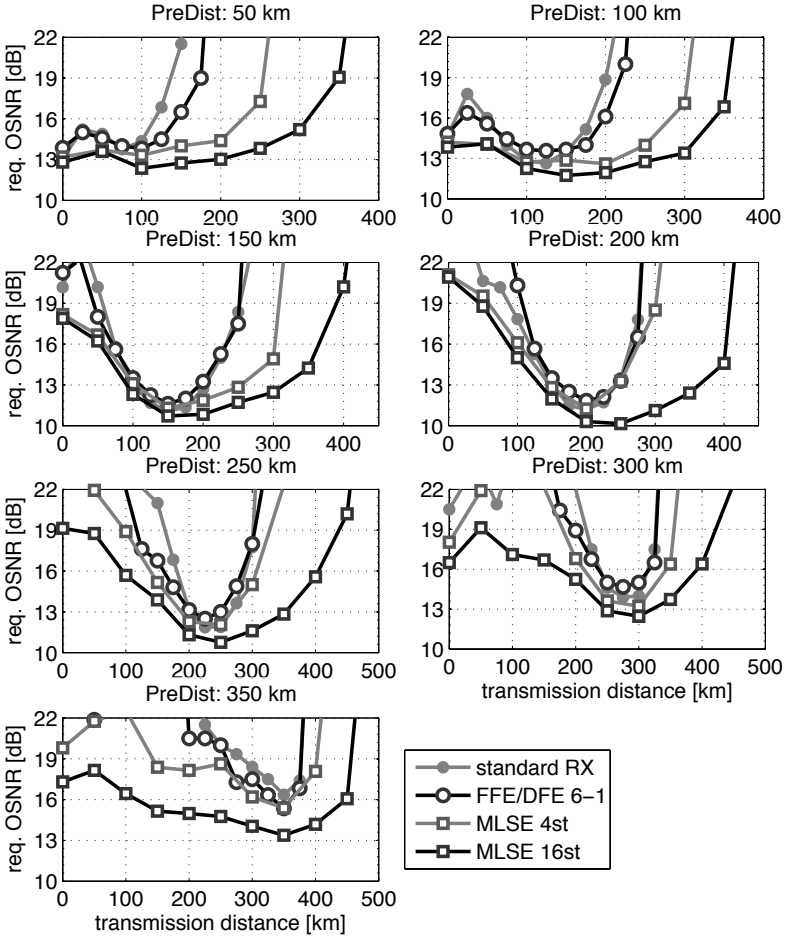

Figure 6.4.: System performance of different predistorted signals in conjunction with an FFE/DFE or MLSE equalizer at the receiver (BER = 10^{-3}).

- The 16 state MLSE also improves the maximum transmission distance for larger initially predistorted signals.
- The dispersion tolerance towards shorter transmission distances as it was predistorted for, is significantly improved by the 16 state MLSE.

In conlusion, mainly the 16 state MLSE may improve the system performance of the predistorted system, while the advantage of the FFE/DFE is not significant. This result is not unexpected, as the purpose of neural net optimization is to find the best predistortion for a non post–equalized system. However, the MLSE significantly improves the transmission performance of the predistorted system and increases the maximum transmission distance by up to 100 km. An optimization of a post–equalized system may further increase the system performance, but is not subject of this work.

CHAPTER 7

SUMMARY AND OUTLOOK

The aim of this work was to study predistortion strategies to overcome the dispersion limit of conventional directly modulated lasers of about 20 km. Calculating a predistorted signal that compensates chromatic dispersion, can be simply done in the optical domain for a complex optical signal. For directly modulated lasers, which are restricted in modulating an arbitrary complex optical signal, the predistortion has to be estimated in the electrical domain and thus a more sophisticated approach is necessary.

Based on a small signal approximation of the optical fiber and the directly modulated laser, it was shown that it is theoretically possible to precompensate the chromatic dispersion with a directly modulated laser. As the small signal approximation is restricted to signals with a low extinction ratio, this approach is not suitable for real optical transmission systems.

Another predistortion technique that was studied in this work were FIR Volterra filters. To overcome the limitation of the linear small signal approximation, a nonlinear FIR Volterra filter is used to compensate chromatic dispersion. It was shown, that a

Volterra filter is capable of compensating the chromatic dispersion at the receiver. In addition to that, the indirect learning algorithm was applied to transfer the Volterra filter from the receiver to the transmitter. Unfortunately, the algorithm was stable only for special system parameters and thus a signal predistortion with FIR Volterra filters could not be obtained.

For the third studied predistortion technique, artificial neural networks as a nonlinear filter and the particle swarm optimization algorithm were used to estimate a signal predistortion. Unlike the first two techniques, the last technique does not estimate a predistorted signal for a given target signal at the receiver, but generates a predistorted signal that minimizes the bit error ratio at the receiver for a given transmission distance. The maximum transmission length in simulations was more than 350 km with an impressive dispersion tolerance of 100 km. Additionally, in experiments with a 2.5 Gbit/s laser modulated at 10 Gbit/s a transmission distance of up to 190 km was shown.

For practical applications it may not be appropriate to use a neural network with dozens of coefficients. Instead it would be suggested to use a look–up table for the predistortion. The advantage of a look–up table is, that any nonlinear system can be easily modeled especially if the memory length is restricted.[1]

Beside the use of directly modulated DFB lasers, the use of VCSEL laser for signal predistortion should be analyzed, as they would help to further reduce the costs. A very promising approach was published by Duong et al. [64]. In an experiment a 10 Gbit/s transmission over 100 km using a 2.5 Gbit/s VCSEL with orthogonal frequency division multiplexing (OFDM) modulation was shown. Here the OFDM modulation is one of the favorites for the challenge to overcome the dispersion limit of directly modulated lasers.

[1] The maximum memory length used for the neural net is 10 taps (5 bit).

APPENDIX A

LASER PARAMETERS

parameter	symbol	value	unit
length of the active area	L_D	$250 \cdot 10^{-6}$	m
width of the active area		$1.8 \cdot 10^{-6}$	m
height of the active area		$0.06 \cdot 10^{-6}$	m
refractive index	n_1	4	
mirror reflectivity	R_1, R_2	0.32	
internal losses	α_{int}	2500	1/m
electron lifetime	τ_e	$1.6 \cdot 10^{-9}$	s
differential gain	a or $\frac{dg_{st}}{dn}$	$3 \cdot 10^{-20}$	m^{-1}
gain compression factor	κ_s	$2.2 \cdot 10^{-7}$	
confinement factor	Γ	0.1	
transparency carrier density	N_0	$1.5 \cdot 10^{24}$	m^{-3}
slope efficiency	η	0.2583	W/A
center frequency	$\nu_t h$	$193.4 \cdot 10^{12}$	Hz
chirp (linewidth enhancement) factor	α_{ch}	1, 2, 3	

APPENDIX B

ABBREVIATIONS

W	energy
P	optical power
E	amplitude of electrical field
N	carrier density
I	laser injection current
S	photon number
ν	frequency of light
t	time
h	Planck constant
N_0	transparency carrier density
N_{th}	threshold carrier density
g	gain coefficient, $g = g_{st}\Gamma$
g_{st}	stimulated gain coefficien, $g_{st} = a(N - N0)$
κ_S	compression factor
Γ	confinement factor
L_D	laser length

V	volume of active region
a	differential gain / cross section
R_1, R_2	reflectivity of the laser cavity
v_g	group velocity of light
t_p	photon lifetime
t_e	electron lifetime
R	recombination rate of the carrier
R_{sp}	spontaneous emission
α_{int}	internal laser losses
α	laser chirp
G	normalized gain, $G = v_g \Gamma \tau_p g_{st}$
G_l	linear normalized gain
ω_g	characteristic angular frequency
ω_r	relaxation resonance angular frequency
ω_d	damping angular frequency
K	modulation K–factor
$H_{LD}(j\omega)$	laser transfer function
n_1, n_2	refractive index of the core and the cladding of a fiber
α_{fib}	fiber loss
α_s	losses due to Rayleigh scattering
L	fiber length
μ_0	vacuum permeability
ε_0	vacuum permittivity
χ	susceptibility
k_0	free space wave number
λ	wavelength
$\vec{r}$	position vector
$\vec{E}$	electrical field
$\vec{P}$	electrical polarization
$\vec{e}_x, \vec{e}_y$	unit vectors in x, y direction
$H'_{LD}(j\omega)$	laser transfer function for the optical intesity
$H_f^{(e)}$	fiber transfer function for the optical power
$H_f^{(o)}$	fiber transfer function for the complex optical signal
f	neural net transfer function

b_m^k	neural net bias coefficient
$w_{m,j}^k$	neural net coefficient
$\vec{v}$	particle velocity
g	inertia parameter
c_1, c_2	cognitive, social parameter
ξ_1, ξ_2	random values
$\vec{P}$	particle (e.g. set of neural net coefficients)
$\vec{P}_{best}$	local optimal particle
$\vec{G}_{best}$	global optimal particle
$J[n]$	fitness function
λ	forgetting factor
$e[n]$	error
p	probability density function
Z	received sequence
U	candidate sequence

BIBLIOGRAPHY

[1] B. Wedding, "New method for optical transmission beyond dispersion limit," *Electronics Letters*, vol. 28, no. 14, pp. 1298–1300, 1992.

[2] D. Mahgerefteh, Y. Matsui, C. Liao, B. Johnson, D. Walker, X. Zheng, Z. Fan, K. McCallion, and P. Tayebati, "Error-free 250 km transmission in standard fibre using compact 10 Gbit/s Chirp–Managed directly modulated lasers (CML) at 1550 nm," *Electronics Letters*, vol. 41, pp. 543 – 544, 2005.

[3] J. McNicol, M. O'Sullivan, K. Roberts, A. Comeau, D. McGhan, and L. Strawczynski, "Electrical domain compensation of optical dispersion," in *Optical Fiber Communication Conference, OFC 2005*, 2005, paper OThJ3.

[4] R. Killey, P. Watts, V. Mikhailov, M. Glick, and P. Bayvel, "Electronic dispersion compensation by signal predistortion using a dual-drive mach-zehnder modulator," in *Optical Fiber Communication Conference, OFC 2005*, 2005, paper OThJ2.

[5] K. Petermann, *Laser Diode Modulation And Noise.* Kluwer Academic Publishers, 1988.

[6] R. Tucker, "High - speed modulation of semiconductor lasers," *IEEE Journal of Lightwave Technology*, vol. LT-3, pp. 1180–1192, 1985.

[7] P. Morton, T. Tanbun-Ek, R. Logan, N. Chand, K. Wecht, A. Sergent, and J. Sciortino, P.F., "Packaged 1.55 μm DFB laser with 25 GHz modulation bandwidth," *Electronics Letters*, vol. 30, no. 24, pp. 2044–2046, 1994.

[8] G. P. Agrawal, *Fiber-Optic Communication Systems.* John Wiley & Sons, 2002.

[9] S. Heather, M. Edwards, and A. Woodfin, "Standard singel mode fieber upgrades to full spectrum and G.652.D," Corning Inc., Tech. Rep., 2004. [Online]. Available: http://www.corning.com/docs/opticalfiber/WP3718.pdf

[10] G. P. Agrawal, *Nonlinear Fiber Optics.* Academic Press, 2001.

[11] M. Bass and E. W. V. Stryland, Eds., *Fiber Optics Handbook, Fiber, Devices and Systems for Optical Communications.* McGraw-Hill, 2002.

[12] D. Marcuse, "Pulse distortion in single-mode fibers. 3: Chirped pulses," *Applied Optics*, vol. 20, no. 20, pp. 3573–3579, 1981.

[13] J. Fells, M. Gibbon, I. White, G. Thompson, R. Penty, C. Armistead, E. Kimber, D. Moule, and E. Thrush, "Transmission beyond the dispersion limit using a negative chirp electroabsorption modulator," *Electronics Letters*, vol. 30, no. 14, pp. 1168–1169, 1994.

[14] T. Saito, N. Henmi, S. Fujita, M. Yamaguchi, and M. Shikada, "Prechirp technique for dispersion compensation for a high-speed long-span transmission," *Photonics Technology Letters, IEEE*, vol. 3, pp. 74–76, 1991.

[15] N. Henmi, T. Saito, and T. Ishida, "Prechirp technique as linear dispersion compensation of ultra-high speed long span intensity modulation directed detection optical communication systems," *IEEE Journal of Lightwave Technology*, vol. 12, pp. 1706–1719, 1994.

[16] I. Tomkos, B. Hallock, I. Roudas, R. Hesse, A. Boskovic, J. Nakano, and R. Vodhanel, "10 Gbit/s transmission of 1.55 μm directly modulated signal over 100 km of negative dispersion fibers," *Photonics Technology Letters, IEEE*, vol. 13, no. 7, pp. 735–737, 2001.

[17] H. Chung, Y. Jang, and Y. Chung, "Directly modulated 10 Gbit/s signal transmission over 320 km of negative dispersion fiber for regional metro networks," *Photonics Technology Letters, IEEE*, vol. 15, no. 9, pp. 1306–1308, 2003.

[18] L.-S. Yan, C. Yu, Y. Wang, T. Luo, L. Paraschis, Y. Shi, and A. Willner, "40 Gbit/s transmission over 25 km of negative-dispersion fiber using asymmetric narrow-band filtering of a commercial directly modulated DFB lasers," *Photonics Technology Letters, IEEE*, vol. 17, no. 6, pp. 1322–1324, 2005.

[19] E. Voges and K. Petermann, Eds., *Optische Kommunikationstechnik*. Springer - Verlag, 2002.

[20] E. W. Weisstein, "de Bruijn Sequence," From MathWorld – A Wolfram Web Resource. [Online]. Available: http://mathworld.wolfram.com/deBruijnSequence.html

[21] P. Morton, G. Shtengel, L. Tzeng, R. Yadvish, T. Tanbun-Ek, and R. Logan, "38.5 km error free transmission at 10 Gbit/s in standard fibre using a low chirp, spectrally filtered, directly modulated 1.55 μm DFB lasers," *Electronics Letters*, vol. 33, no. 4, pp. 310–311, 1997.

[22] S. Mohrdiek, H. Burkhard, F. Steinhagen, H. Hillmer, R. Losch, W. Schlapp, and R. Gobel, "10 Gitb/s standard fiber transmission using directly modulated 1.55 μm

quantum-well DFB lasers," *Photonics Technology Letters, IEEE*, vol. 7, no. 11, pp. 1357–1359, 1995.

[23] B. Wedding, B. Franz, and B. Junginger, "10 Gbit/s optical transmission up to 253 km via standard single-mode fiber using the method of dispersion-supported transmission," *IEEE Journal of Lightwave Technology*, vol. 12, no. 10, pp. 1720–1727, 1994.

[24] B. Wedding, W. Pohlmann, B. Franz, and H. Geupel, "Multilevel dispersion supported transmission at 20 Gbit/s over 46 km installed standard singlemode fibre," in *European Conference on Optical Communication, ECOC 1996*, 1996, paper MoB.4.4.

[25] B. Wedding, W. Idler, B. Franz, W. Pohlmann, and E. Lach, "40 Gbit/s quaternary dispersion supported transmission over 31 km standard singlemode fibre without optical dispersion compensation," in *European Conference on Optical Communication, ECOC 1998*, vol. 1, 1998, pp. 523 – 524.

[26] D. Mahgerefteh and F. Fan, "Chirp-managed-laser technology delivers > 250 km reach," *Lightwave Online*, 2005. [Online]. Available: http://www.finisar.com/download_31wMeaCML_Application%20White%20Paper-LW.pdf

[27] I. P. Kaminow, T. Li, and A. E. Willner, *Optical fiber telecommunications V B, Systems and networks.* Academic Press, Jan 2008.

[28] D. Mahgerefteh, Y. Matsui, X. Zheng, Z. Fan, K. Mccallion, and P. Tayebati, "Chirp managed laser CML: A compact transmitter for dispersion tolerant 10 Gbit/s networking applications," in *Optical Fiber Communication Conference, OFC 2006*, 2006, paper OWC6.

[29] D. McGhan, C. Laperle, A. Savehenko, C. Li, G. Mak, and M. O'Sullivan, "5120 km RZ–DPSK transmission over

G.652 fiber at 10 Gbit/s with no optical dispersion compensation," in *Optical Fiber Communication Conference, OFC 2005*, 2005, paper PDP27.

[30] Nortel, "Breaking the physical barriers with electronic dynamically compensating optics (eDCO)," Nortel, Tech. Rep., 2006. [Online]. Available: http://www.nortel.com/solutions/optical/collateral/nn115923.pdf

[31] J. Wang and K. Petermann, "Small signal analysis for dispersive optical fiber communication systems," *IEEE Journal of Lightwave Technology*, vol. 10, pp. 96–100, 1992.

[32] S. Haykin, *Neural Networks. A Comprehensive Foundation*, 2nd ed. Prentice Hall, 1999.

[33] M. M. E. Said, J. Sitch, and M. I. Elmasry, "An electrically pre-equalized 10 Gbit/s duobinary transmission system," *IEEE Journal of Lightwave Technology*, vol. 20, pp. 388–400, 2005.

[34] S. Haykin, *Adaptive Filter Theory*, 3rd ed. Prentice Hall, 1996.

[35] O. Agazzi, D. Messerschmitt, and D. Hodges, "Nonlinear echo cancellation of data signals," *Transactions on Communications, IEEE*, vol. 30, no. 11, pp. 2421–2433, 1982.

[36] S. Benedetto, E. Biglieri, and R. Daffara, "Modeling and performance evaluation of nonlinear satellite links - a volterra series approach," *Transactions on Aerospace and Electronic Systems, IEEE*, vol. AES-15, no. 4, pp. 494–507, 1979.

[37] G. Sicuranza, A. Bucconi, and P. Mitri, "Adaptive echo cancellation with nonlinear digital filters," in *IEEE International Conference on Acoustics, Speech, and Signal Processing, ICASSP 1984.*, vol. 9, 1984, pp. 130 – 133.

[38] C. Xia and W. Rosenkranz, "Nonlinear electrical equalization for different modulation formats with optical filtering," *IEEE Journal of Lightwave Technology*, vol. 25, no. 4, pp. 996–1001, 2007.

[39] W. J. Rugh, *Nonlinear System Theory - The Volterra/Wiener Approach*. Originally published by The Johns Hopkins (Web version prepared in 2002), 1981.

[40] V. Mathews, "Adaptive polynomial filters," *Signal Processing Magazine, IEEE*, vol. 8, no. 3, pp. 10–26, 1991.

[41] C. Eun and E. Powers, "A new volterra predistorter based on the indirect learning architecture," *Transactions on Signal Processing, IEEE*, vol. 45, no. 1, pp. 223–227, 1997.

[42] K. Hornik, "Approximation capabilities of multilayer feedforward networks," *Neural Networks*, vol. 4, no. 2, pp. 251–257, 1991.

[43] P. Miller, "Swarm theory," *National Geographic*, July 2007. [Online]. Available: http://ngm.nationalgeographic.com/2007/07/swarms/miller-text

[44] T. Weise, *Global Optimization Algorithms*, 2nd ed. http://www.it-weise.de/, 2008.

[45] J. Kennedy and R. C. Eberhart, *Swarm Intelligence*. Morgan Kaufmann Publishers, 2001.

[46] J. Kennedy and R. Eberhart, "Particle swarm optimization," in *IEEE International Conference on Neural Networks, 1995*, 1995, pp. 1942–1948.

[47] S. Randel, "Analyse faseroptischer Übertragungssysteme mit wellenlängenmultiplex bei 160 Gbit/s Kanaldatenrate," Dr.-Ing, Technische Universität Berlin, 2005.

[48] R. N. McDonough and A. D. Whalen, *Detection of Signals in Noise*, 2nd ed. San Diego: Academic Press, 1995.

[49] J. Nocedal and S. J. Wright, *Numerical Optimization*, 2nd ed. Springer, 2006.

[50] C. Kurtzke and A. Gnauck, "Operating principle of inline amplified dispersion-supported transmission," *Electronics Letters*, vol. 29, no. 22, pp. 1969 – 1971, Sep 1993.

[51] I. Papagiannakis, C. Xia, D. Klonidis, W. Rosenkranz, A. N. Birbas, and I. Tomkos, "Performance of 2.5 Gbit/s and 10 Gbit/s transient and adiabatic chirped directly modulated lasers using electronic dispersion compensation," in *European Conference on Optical Communication, ECOC 2007*, 2007.

[52] *802.3aq-2005 (10GBASE-LRM)*, IEEE Standards Association Std. [Online]. Available: http://standards.ieee.org/getieee802/download/802.3aq-2006.pdf

[53] T. Nielsen and S. Chandrasekhar, "OFC 2004 workshop on optical and electronic mitigation of impairments," *IEEE Journal of Lightwave Technology*, vol. 23, no. 1, pp. 131–142, 2005.

[54] F. Buchali, H. Bülow, W. Baumert, R. Ballentin, and T. Wehreu, "Reduction of the chromatic dispersion penalty at 10 Gbit/s by integrated electronic equalisers," in *Optical Fiber Communication Conference, OFC 2000*, 2000, paper ThS -1.

[55] J. Winters and R. Gitlin, "Electrical signal processing techniques in long-haul fiber-optic systems," *Transactions on Communications, IEEE*, vol. 38, no. 9, pp. 1439–1453, 1990.

[56] A. Faerbert, S. Langenbach, N. Stojanovic, C. Dorschky, T. Kupfer, C. Schulien, J. Elbers, H. Wernz, H. Griesser, and C. Glingener, "Performance of a 10.7 Gbit/s receiver with digital equaliser using maximum likelihood sequence estimation," in *European Conference on Optical Communication, ECOC 2004*, 2004, paper PD-Th4.1.5.

[57] O. Agazzi, M. Hueda, H. Carrer, and D. Crivelli, "Maximum-likelihood sequence estimation in dispersive optical channels," *IEEE Journal of Lightwave Technology*, vol. 23, no. 2, pp. 749–763, Feb. 2005.

[58] O. Agazzi and V. Gopinathan, "The impact of nonlinearity on electronic dispersion compensation of optical channels," in *Optical Fiber Communication Conference, OFC 2004*, 2004, paper TuG6.

[59] B. Sklar, "How I learned to love the trellis," *Signal Processing Magazine, IEEE*, vol. 20, no. 3, pp. 87–102, 2003.

[60] A. Viterbi, "Error bounds for convolutional codes and an asymptotically optimum decoding algorithm," *Transactions on Information Theory, IEEE*, vol. 13, no. 2, pp. 260 – 269, Jan 1967.

[61] J. Forney, G., "Maximum-likelihood sequence estimation of digital sequences in the presence of intersymbol interference," *Transactions on Information Theory, IEEE*, vol. 18, no. 3, pp. 363–378, 1972.

[62] M. Feuer, S.-Y. Huang, S. Woodward, O. Coskun, and M. Boroditsky, "Electronic dispersion compensation for a 10 Gbit/s link using a directly modulated lasers," *Photonics Technology Letters, IEEE*, vol. 15, no. 12, pp. 1788–1790, 2003.

[63] C. Fludger, J. Whiteaway, and P. Anslow, "Electronic equalisation for low cost 10 Gbit/s directly modulated systems," in *Optical Fiber Communication Conference, OFC 2004*, 2004, paper WM7.

[64] T. Duong, N. Genay, P. Chanclou, and B. Charbonnier, "10 Gbit/s transmission over 2.5 GHz bandwidth by direct modulation of commercial VCSEL and multi-mode FP lasers using adaptively modulated optical OFDM modulation for

passive optical networks," in *European Conference on Optical Communication, ECOC 2008*, 2008, paper We.1.F.4.

BIBLIOGRAPHY

[Warm1] S. Warm, C.-A. Bunge, T. Wuth, K. Petermann "Electronic Dispersion Precompensation With a 10-Gb/s Directly Modulated Laser", *IEEE Photon. Technol. Lett.*, Vol. 21, No. 15, pp. 1090-1092, Aug. 2009.

[Warm2] S. Warm, C.-A. Bunge, T. Wuth, K. Petermann "Electronic Dispersion Precompensation Using a Directly Modulated Laser", *Proc. ECOC 2008*, P.4.07, Brüssel, Belgien, Sept. 2008.

[Warm3] S. Warm, C.-A. Bunge, T. Wuth, K. Petermann "Elektronische Vorkompensation der chromatischen Dispersion in faseroptischen Übertragungssystemen mit alleiniger Verwendung eines direkt modulierten Lasers", *Proc. 8. ITG-Fachtagung Photonische Netze*, pp. 105-108, Leipzig, Mai 2007.